This project has received funding from the Euratom research and training programme 2014-2018 under grant agreement No 662287.

EJP-CONCERT

European Joint Programme for the Integration of Radiation Protection Research

H2020 – 662287

D9.16 – Evaluation of the importance of radioactive particles in radioecological models

Authors: Ole Christian Lind, Justin Brown, Ali Hosseini, Brit Salbu, Valery Kashparov, Nicholas Beresford

Reviewer(s): W. Raskob
and CONCERT coordination team

Work package / Task	**WP9** **T9.1**	**ST 9.1.3**
Deliverable nature:	**Report**	
Dissemination level: (Confidentiality)	**Public**	
Contractual delivery date:	**M53**	
Actual delivery date:	**M53**	
Version:		
Total number of pages:	**58**	
Keywords:	**Food-chain model; ECOLEGO; U fuel particles, weathering; transfer; crops**	
Approved by the coordinator:	**M54**	
Submitted to EC by the coordinator:	**M54**	

Author affiliations
Lind, O-C., Salbu, B. - *Norwegian University of Life Sciences (NMBU; Norway)*
Brown, J.E., Hosseini, A, - *Norwegian Radiation Protection Authority (NRPA; Norway)*
Kashparov, V. - National University of Life and Environmental Sciences of Ukraine
Beresford, N.A. - *Centre for Ecology & Hydrology (CEH; United Kingdom)*

Reviewer affiliation: Raskob, W. - *Karlsruhe Institute of Technology (KIT; Germany)*

Abstract

History has shown that radioactive particles are released to the environment following severe nuclear events. This report describes the adaptation of the particle concept into the FDMT food chain model, in particular the implementation of uranium (U) fuel particles and their influence on bioavailability and soil to plant transfer of ^{137}Cs and ^{90}Sr. A bespoke compartmental model has been conceptualized based upon an understanding of particle characteristics and behavior, based on comprehensive particle archives and associated data bases. Parameters, such as those describing particle weathering rates being essential for transfer rates between compartments (representing e.g. soil solution and reversibly bound radionuclides) and leaching rates from soils have been derived from lab and field experiments. The model parametrization of U fuel particle weathering rates, which strongly depend on soil pH and solid-state speciation of the carrying matrix (i.e., oxidized or non-oxidized UO_2 fuel particles, or U transformed to extra inert forms such as UZr_xO_y probably due to interactions with zircalloy) was based on extensive data sets from the Chernobyl exclusion zone. Furthermore, the implementation of U particles and restructuring of FDMT within a model development platform allowed the default soil radionuclide transfer model to be replaced with this new particle soil model. The semi-mechanistic 'Absalom model' has also been considered as an alternative for predicting soil to plant transfer. Scenarios have been developed to explore the influence of particle composition and soil acidity on radionuclide bioavailability and food-chain transfer (to crops, grass and cow-milk). There appear to be substantial differences in the predictions made for transfer of radionuclides to selected foodstuffs between the new particle soil model, the current FDMT and the Absalom model. The new particle soil model predicts a delay in the maximum levels observed in food-chains (excluding the initial few months post deposition), a result that appears more congruent with observations for areas close to the reactor. The model output data were compared with time-series of ^{137}Cs and ^{90}Sr in grain crops from the Ivankiv district just south of the Chernobyl exclusion zone. The results showed that the revised model, considering radioactive particle weathering and soil migration processes, in some respects, exhibited improved prediction capabilities compared to the current FDMT model, especially in the long-term after deposition. However, the current version of the revised model tends to under-predict both ^{137}Cs and ^{90}Sr activity concentrations in grain, although the simulated values are of the same order of magnitude as empirical determinations. The results encourage further development of the new particle model by including processes involved during the early stages (weeks and months) post-accident focussing the above ground part of the atmosphere-plant-soil system. Such processes might include deposition, interception, transformation and subsequent transportation of particles and associated remobilized radionuclides at the interface of atmosphere and the soil-water -plant compartment.

Table of Contents

1 Introduction

1.1 Background and aims

Radioecological simulation models used to predict the transfer of radionuclides along the food chain are associated with considerable uncertainties. In the initial phase after a nuclear accident, the factors determining the contamination of foodstuffs will largely be defined by vegetation interception and the time of year. Factors controlling the uptake of radionuclides to vegetation from soil will become more important during the transition phase and they will subsequently dominate in the long-term rehabilitation phase. However, predictions made using radioecological models will be used in the early part of the transition phase to make longer-term decisions, e.g., with regard to remediation strategies. Therefore, models must be sufficiently robust and fit for purpose with uncertainties reduced where practicable.

Following severe nuclear events, however, a major fraction of refractory radionuclides will be released as radioactive particles, containing fission and activation products such as ^{90}Sr and ^{137}Cs as well as transuranics. Chernobyl particles were first observed in samples collected during deposition in April-May 1986 in the near field as well as in air filters from Sweden (Devell et al., 1986) and in ultra filtered rainwater in Norway May 1986 (Salbu, 1988), about 2,000 km away from the source. After the Chernobyl accident, 6-8 different particle classes have been identified, having different composition and characteristics (Kashparov et al., 2004b; Kashparov et al., 1999b; Kashparov et al., 2000b; Salbu et al., 2018). According to a recent summary of lessons learned from the Chernobyl accident, "one of the areas being significantly advanced" since 1986 was the characterization and environmental behaviour of hot particles" (Beresford et al., 2016).

In the present work, focus has been put on uranium (U) fuel particles (FP). Based on many years of research as well as a comprehensive particle archive and detailed data bases, the fuel particles could be divided into 3 groups according to the particle properties (size, crystalline structure and oxidation state) and weathering/dissolution rates under natural conditions (Kashparov et al., 2004a; Kashparov et al., 1999a; Kashparov et al., 2000b):

1. Chemically extra-stable U-Zr-O particles depleted in volatile radionuclides were formed as a result of high-temperature annealing of UO_2 in the presence of zirconium containing construction material. These particles were released during the initial explosion and deposited to the West of the reactor, for instance in Scandinavia,
2. Non-oxidized chemically stable UO_2 fuel particles present in the initial release were formed due to mechanical destruction of nuclear fuel. These relative inert particles were also deposited along the narrow western trace of fallout.
3. Oxidized U particles (UO_{2+x} particles) having low chemical stability were formed as a result of the fire. These particles were predominantly deposited to the North and South of the reactor.

All three types of fuel particles were observed in the initial fallout. The relative contribution varied, however, depending on the direction and distance from the ChNPP as well as on the degree of interaction with Zr and on the degree of oxidation.

Soils and sediments can act as a sink for deposited particles, and, following deposition, these particle contaminated soils and sediments may also act as potential diffuse sources in the future (Salbu et al.,

2018). Thus, knowledge with respect to particle characteristics and processes influencing particle weathering, i.e., the transformation of solid state radionuclide species bound in a particle matrix to dissolved species, information on potentially bioavailable forms (Kashparov et al., 2004) is needed to assess long-term impact from radioactive particle contamination. The biological uptake (initially via root uptake) of particle-associated radionuclides will be delayed until particle weathering and remobilisation of associated radionuclides occur. The apparent radionuclide soil-water distribution coefficient (K_d) can be extremely high (many orders of magnitude) if high activity particles are retained in soils (Salbu et al., 2018; Salbu et al., 2004), and due to weathering the apparent K_d will change over time as particle-associated radionuclides become more mobile . It has been suggested that to reduce uncertainty in transfer estimates, the steady-state concept should be replaced with a rate function describing particle weathering (Salbu, 2018).

The main focus of this work was the adaptation of the particle concept into the FDMT model, implementing fuel particles into the food chain transfer module of the JRodos decision support system (Brown et al., 2018) to account for the presence of particles deposited in the environment, and to determine if predictions are likely to be significantly impacted by the presence of particles or not. To include radioactive particles in transfer models, information on particle characteristics such as composition, weathering rates and remobilization potential of associated radionuclides is needed.

With the aim of assessing the potential importance of particle-associated radionuclides in model predictions, the objectives of the present work were to:

- Develop the ECOLEGO implementation of the FDMT[1] model (as described by Brown et al. 2018) to include descriptions of particle characteristics such as weathering and particle soil migration processes
- Test the revised model and compare model outputs with the those from the standard FDMT model
- Evaluate the revised model by comparing with field observation data.

Data on particle characteristics was based on information from radioactive particle archives in Ukraine (NuBiP) and Norway (NMBU) and from extensive data bases obtained from the Chernobyl Exclusion Zone over the last three decades (Kashparov et al., 2019). This work was focussing on the influence of particle behaviour on soil – water relationship (Kd) and soil to plant transfer modelling of ^{137}Cs and ^{90}Sr due to their importance for dosimetry and impact assessments as well as due to readily available data sets.

2 Description of the FDMT and ECOLEGO models

There are many radionuclide food-chain transfer models that have been developed over the last few decades most of which may be adaptable to requirements for simulating the behaviour and fate of radioactive particles in the environment. Here we have used the FDMT (Food Chain and Dose Module for Terrestrial Pathways) model which was developed under European funding and is used by about 20 European states (Raskob et al., 2018). As noted in (Brown et al., 2018), FDMT, as described by (Müller et al., 2004), has been implemented in both the "Real-time On-line Decision Support System" (RODOS/JRodos) (Levdin et al., 2010) and the “Accident Reporting and Guiding Operational System”

[1] Hereafter referred to as FDMT/ECOLEGO

(ARGOS) (Hoe et al., 2008). FDMT allows predictions of radionuclide activity concentrations over time in various, mainly agricultural, food products for given inputs of radionuclides into geographically-specified terrestrial systems to be made. The module, additionally, allows doses to members of the public via relevant pathways including internal exposure (from ingestion and inhalation) and external exposure (from plume passage and deposited radionuclides) to be derived. A key assumption that lies behind FDMT is that inputs to the system occur in the form of aerosols (the exception being radioiodine where elemental, organic bound and aerosol fractions can be defined separately).

FDMT is largely based upon the earlier dynamic model ECOSYS-87 (Müller and Pröhl, 1993) that was originally implemented within Microsoft EXCEL™. Much of the developmental work including the numerical specification of many of the parameters used in ECOSYS-87 (and therefore FDMT) was completed in the 1980s and hence many of the later, large numbers of radioecology studies prompted by the 1986 Chernobyl accident were not considered. This latter shortcoming has now been considered within CONFIDENCE (Brown et al., 2018) and elsewhere (Staudt, 2016 ; Thørring et al., 2016).

As described in (Brown et al., 2018), there are numerous limitations associated with the FDMT model as incorporated within the JRodos and ARGOS decision support systems. This provided the rationale for extracting the model and implementing it within a probabilistic-enabled modelling platform called ECOLEGO. In so doing, the possibility to be more flexible in terms of incorporating new components and sub-models was introduced further enabling an exploration of the factors that introduce variability within model predictions. ECOLEGO is a modelling platform for creating dynamic models and performing deterministic or probabilistic simulations ((Avila et al., 2005); http://ecolego.facilia.se/ecolego/show/HomePage). The software incorporates powerful numerical solvers for complex and dynamic systems (i.e. solver for ordinary differential equations including 'stiff' problems) and provides support for probabilistic simulations using Monte Carlo or Latin Hypercube sampling.

The earlier CONFIDENCE deliverable (Brown et al., 2018) describes how ECOSYS-87/FDMT was incorporated within ECOLEGO allowing for modification of sub-models and probabilistic simulation. The report also provides details on testing and quality assurance of the ECOSYS-87/FDMT implementation on the ECOLEGO platform through comparison with the existing model configuration for given cases. The collation of relevant and up-to-date statistical information for identified (primarily element-dependent/radioecological) parameters was described and outputs (based on the statistical collations) from the new version of the model on the modelling platform with those from the old (default parameter) version of the model were compared.

This earlier effort now provides the foundation for the work described in this deliverable report; the FDMT/ECOLEGO version with updated parameter values (largely based upon IAEA (2010) and a review of farm animal biological half-lives conducted by CONFIDENCE (Barnett et al., 2019) is used.

2.1 Which parts of the FDMT model may need to be modified to account for the presence of radioactive particles?

As noted by Brown et al. (2018), various parameters used in FDMT could be influenced by the presence of particles. These include:

- Deposition velocities, which will change as a function of particle size and density (and physico-chemical form). There is also a link to canopy interception and retention of radionuclides including radioactive particles to different plant types
- Loss from the vegetation canopy (weathering rates) which will presumably be affected by particle characteristics
- Radionuclide root uptake which is likely to be affected by the presence of particles
- Translocation from the leaves to the edible part of the plant
- Feed to animal transfer coefficients (radionuclide Bq/kg in animal per Bq/day ingested), which may be affected by the presence of particles.

From a practical perspective of there being very little published information enabling parameterization for the abovementioned list, focus has been placed on making developments in relation to the soil processes model which will be the most important component of the model determining long-term behaviour. As (Brown et al., 2018) identified adaptation of the model would need to consider how to include particle composition and the weathering of particles and the associated mobilisation of radionuclides over time.

Distribution of radionuclides in soil system

The distribution of radionuclides in soil systems with respect to potential different physico-chemical forms of radioactive fallout, and uptake by plants can be described by a model such as that illustrated below (Figure 1).

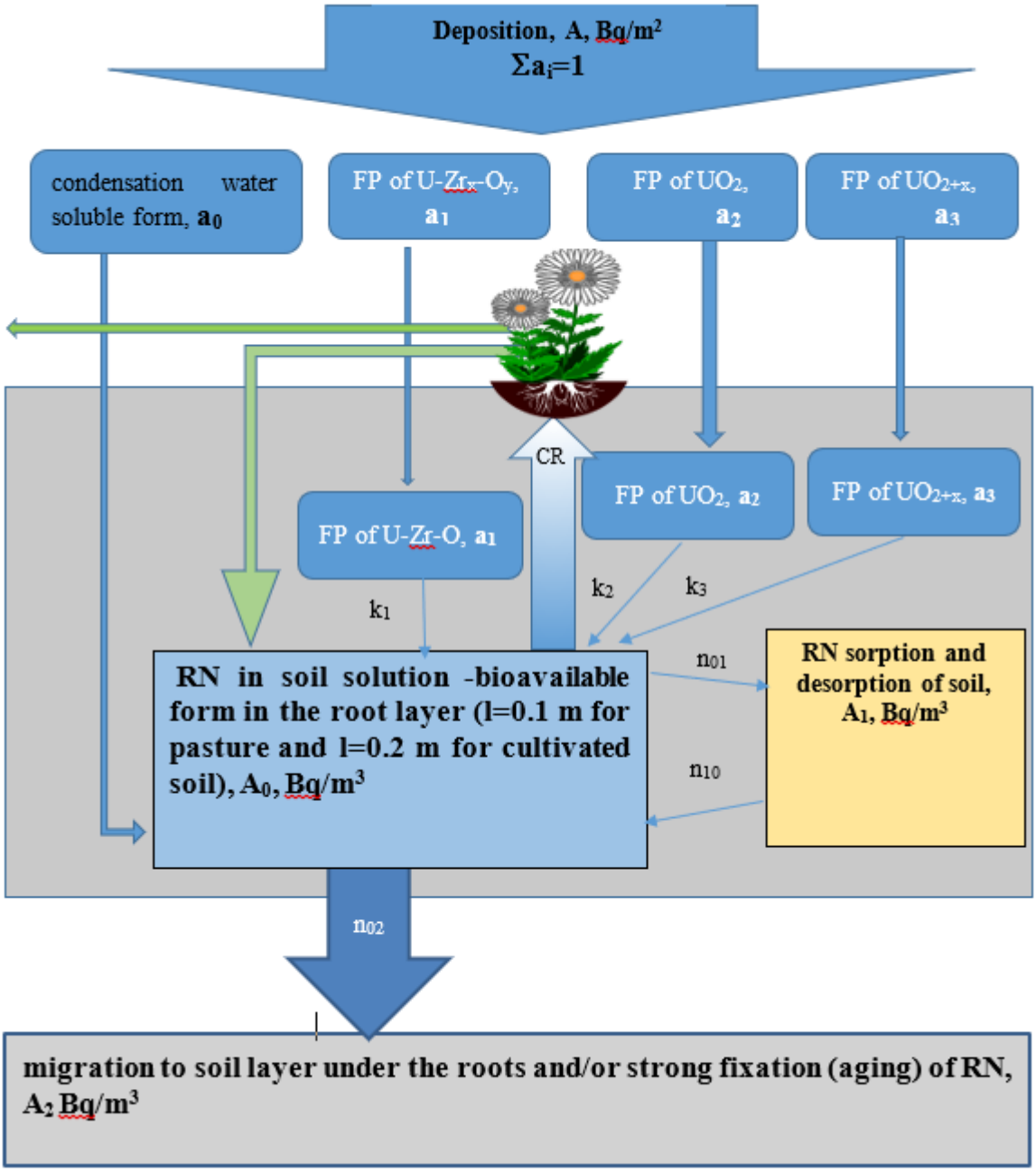

Figure 1. Conceptual basis for modeling deposition and plant uptake of radionuclides (RNs). "Condensation water soluble form, a_0" type particles refer to particles that have been formed from condensation of volatilized radionuclides during a high temperature release scenario with an assumed 100% water solubility.

Particle weathering and transfer of radionuclides from solid state particle-associated forms to potentially bioavailable dissolved forms can be described according to:

$$\begin{cases} \frac{\partial A(t)}{\partial t} = -A(a_1k_1 + a_2k_2 + a_3k_3 + \lambda) & (1) \\ \frac{\partial A_0(t)}{\partial t} = A/l\,(a_1k_1 + a_2k_2 + a_3k_3) - (n_{01} + n_{02} + \lambda)\cdot A_0 + n_{10}A_1 & (2) \\ \frac{\partial A_1(t)}{\partial t} = n_{01}A_0 - (n_{10} + \lambda)\cdot A_1 & (3) \\ \frac{\partial A_2(t)}{\partial t} = n_{02}A_0 - \lambda A_2 & (4) \end{cases}$$

Where (Fig.1) A – density of radionuclides deposition, Bq·m^{-2};

A_0- activity concentration of radionuclides in soil solution -bioavailable form of RN, Bq·m^{-3};

A_1- activity concentration of radionuclides in sorbed form in soil, Bq·m^{-3};

A_2- activity concentration of radionuclides in an irreversibly sorbed form in the soil (or migrated from the root layer), Bq·m^{-3};

a_i –**(Σa_i=1)** part of particle type (i=0 for water soluble form of RN fallout; i=1 for RN in matrix of of U-Zr_x-O_y, particles; i=2 for RN in matrix of of UO_2, particles; i=3 for RN in matrix of UO_{2+x} particles;) with weathering rate k_i , year^{-1};

n_{01}, n_{10}, n_{02} – rate constants of RN sorption from soil solution, desorption to soil solution and irreversibly sorption from soil solution (or migrated from the root layer), year^{-1};

λ – radioactive decay constant of RN, year^{-1};

l –depth of the root layer, m (l=0.1 m for pasture and l=0.2 m for cultivated soil)

With initial conditions at t = 0

$$\begin{cases} A(0) = a_0 \cdot A & (5) \\ A_0(0) = a_0 \cdot A/l & (6) \\ A_i(0) = 0 & (7) \end{cases}$$

In the basic FDMT model, radionuclide activity concentrations in soil are modelled by accounting for post-depositional processes, these being:

- migration/leaching of the radionuclide out of the rooting zone
- fixation in soil and
- subsequent desorption.

The equations governing the behaviour of radionuclides in soil are the analytical solution to a system comprising of two compartments, representing the activity available and not available (fixed) for plants, with transfers (as rate constants representing the three processes above) between and from the compartments (Müller et al., 2004). As default values, the desorption rate is set to zero in FDMT and fixation rates of 2.2×10^{-4} d^{-1} for Cs and 9×10^{-5} d^{-1} for Sr are assumed (although it is noted that the provenance of these values is unclear). For other elements, fixation is considered to be of minor importance and is set to zero.

The processes described above are clearly important and it was, therefore, considered necessary to retain their mathematical representation in any new version of the model. Nonetheless, it was anticipated that the equations governing the system could be removed within the ECOLEGO environment and replaced using explicit compartments, corresponding to soil components, and transfers, using rate constants, between these compartments. In this way, the system could be developed to be more transparent, facilitating the adaptation of the model with the inclusion of particles.

3 Methods

3.1 Collation of Experimental and field data

Radioactive particles are formed due to critical (e.g., explosions) or subcritical (e.g., corrosion processes) destruction of weapon and fuel matrices, or other nuclear or radiological materials. In reactor accidents scenarios involving high temperature and high pressure, solid fuel materials can liquefy, and volatile radionuclides escape (IAEA, 2011, Salbu et al., 2018). Thus, refractory transuranics, fission and activation products remain associated with the fuel material and will be retained particles once liquefied material solidifies. In contrast, particle will be depleted in volatiles. The composition of particles released during the Chernobyl explosion reflected the specific source (e.g., the specific reactor fuel) with respect to U-enrichment, burn-up, and composition of refractory elements, while the release conditions (explosion: high temperature, high pressure, no air; fire: moderate temperature, normal pressure and the presence of air) reflected particle properties such as particle size distribution, crystallographic structures, oxidation states of matrices) (Salbu et al., 2018). Thus, the formation and release of radioactive particles from the Chernobyl unit 4 reactor were an essential ingredient of the Chernobyl source term, representing the starting point of transfer, dose and assessment models, as described in detail below.

Formation of Chernobyl fuel particles (FP)

The nuclear fuel used in the Chernobyl unit 4 reactor was manufactured by powder metallurgy. The UO_2 powder was sintered at high temperature, up to 1750ºC, and at high pressure in a hydrogen atmosphere. The activity (mass/ volume) of the particles is distributed according to the lognormal law:

$$f(r) = \frac{1}{\sqrt{2\pi \cdot r \cdot s}} e^{\frac{1}{2}\left[\frac{\ln(r)-m}{s}\right]^2} \qquad (8)$$

where r is radius of particles (μm); m is the logarithmic mean of the particles radii and s is standard deviation of m (log particles radius). The parameters of this probability distribution have a well-known

physical meaning. The particles radius median equals:

$$R_m = \exp(m) \quad (9)$$

Typical median radii for UO_2 grains (crystallites) in UO_2 nuclear fuel after fabrication in Russia/USSR was 3-4 µm (and the density 10.6±0.1 g cm^{-3}. The size of the grains varies during the operation of the reactor due to the high temperature gradient in the fuel pellet. Due to mechanical destruction (explosion, dramatic energy release, contact with coolant, etc.) and oxidation in the presence of air (Figure 2), the nuclear fuel in the Chernobyl number 4 reactors was destroyed and the sizes of radioactive particles released followed a lognormal distribution (Kashparov et al., 2000a; Shevchenko, 2004).

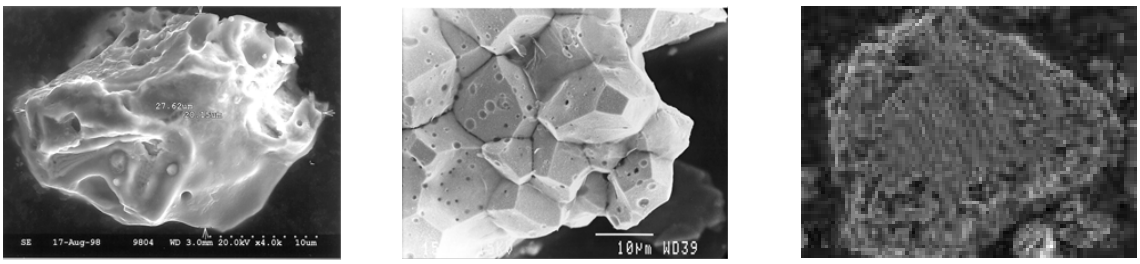

U-Zr_x-O_y **UO_2** **UO_{2+x}**

Figure 2. Uranium fuel particles released from the Chernobyl reactor (Zhurba et al., 2009).

Formation of UZr_xO_y fuel particles

Chemically extra-stable UZr_xO_y particles were formed as a result of high temperature and pressure annealing (>1850ºC, no air present) of UO_2 in presence of zirconium in fuel caging. These particles were formed during the initial explosion (26.04.86) and were transported and deposited within a narrow western trace. Although the size distribution of these UZr_xO_y particles has not been properly studied, the median radius is estimated to have exceeded 10 µm. As a consequence of their size, the fraction of the UZr_xO_y particles in the radioactive fallout rapidly decreased with distance from the source compared with UO_2 FP (Kashparov et al., 2000b). The average relative releases of ^{90}Sr and ^{137}Cs from the fuel during the formation of UZr_xO_y were 23% and 67%, respectively (Kashparov, 2009a), i.e. ^{90}Sr and ^{137}Cs in the UZr_xO_y particles were depleted by approximately 77 % and 33 % compared to fuel.

Formation of UO_2 fuel particles

Chemically stable UO_2 fuel particles initially released on 26.04.86 were formed as a result of mechanical destruction of the nuclear fuel. These particles created the narrow 'western trace' of fallout (Kashparov, 2009a; Kashparov et al., 2003). In order to provide statistically robust data for particle characteristics such as size distribution and water solubility, laboratory experiments were performed in which small pieces of UO_2 from the irradiated undestroyed Chernobyl nuclear fuel were mechanically cracked from a UO_2 pellet and were used as "the initial samples" in thermodynamic experiments. These experiments were initiated to determine the composition of fuel particles after the mechanical destruction of irradiated nuclear fuel (UO_2 particles) and after oxidation of nuclear fuel in the presence of air at different temperatures (400-900ºC) during 3-21 hours (Kashparov et al., 2019; Kashparov et al., 1996; Kashparov et al., 2000b). The uranium dioxide had a burnup 6.5±0.9 MW

day/kg, a $^{235}U/^{238}U$ ratio of 0.0143 ±0.0017, a density of 10.5±0.9 g/cm^3 and the activity concentration on 26 April 1986 of 650±90 MBq/g for ^{90}Sr and 770±50 MBq/g for ^{137}Cs.

UO_2 particles with a median radius of R_m=4.7 µm (s=0.6) were formed as a result of mechanical destruction of irradiated nuclear fuel (Figure 3). The relative fraction (%) of activity of ^{137}Cs and ^{90}Sr associated with condensation[2] particles were 3.3 % and 2.3 %, respectively.

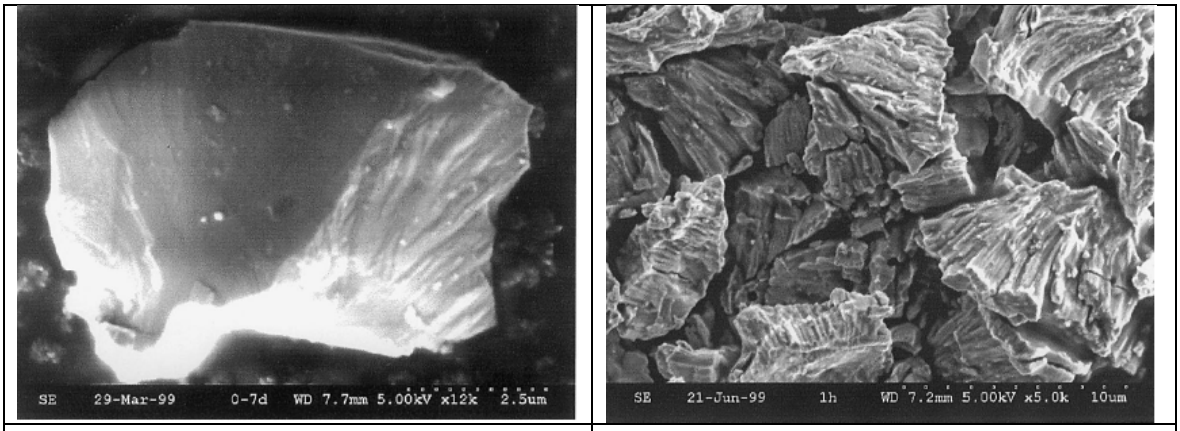

a b

Figure 3. Scanning electron micrograph (SE-mode) of a) particles obtained by crushing nuclear fuel and b) particles obtained after annealing of UO_2 in air at a temperature of 400ºC for 1 h (b).

Formation of UO_{2+x} fuel particles and water soluble condensation particles

Chemically unstable fuel particles (UO_{2+x}) were formed as a result of oxidization of nuclear fuel and were released during the fire over the period 26.04.86-5.05.86. These particles constituted the major part of the fuel particle fallout in the 'Northern and Southern traces' (Kashparov et al., 2004b). In order to provide statistically robust data for particle characteristics such as size distribution and water solubility, laboratory experiments were performed in which original UO_2 fuel was annealed to mimic the conditions during the fire in the Chernobyl reactor.

After 3-21 h of annealing UO_2 fuel in air even at 400-900ºC, the samples of nuclear fuel collected from the Chernobyl Unit 4 reactor were reduced to fine particles or commensurate with the size of UO_2 grains or as grain conglomerates in fuel with median radius of 3-10 µm (Figure 2b, Table 1) (Kashparov et al., 1996; Kashparov et al., 2003). The composition and size distribution of particles formed after annealing were determined by sedimentation in water, by measuring the total activity with a detector with a slot collimator (Kashparov, 2009b), and by image analysis system using BioScan Optimate software in a mode involving automatic step-by-step scanning of the filter surface (Kashparov et al., 1996). For all t and T value sets used in the experiments, t = 3 to 21 h and for a range of T = 400 to 900 C, the particle size distributions could well be described as regular lognormal distribution (eq. 1).

As a result of oxidation of irradiated nuclear fuel, oxidized U particles (e.g. UO_{2+x}) were formed with a log-normal distribution of radii, as showed in Table 1 (Kashparov, 2009b; Kashparov et al., 1996).

[2] Condensation particles are particles that have been formed from condensation of volatilized radionuclides during a high temperature release scenario with an assumed 100% water solubility.

The size distribution of the formed oxidized U fuel particles were relatively independent of temperature in the range of 400-900ºC (Table 1). However, the time of annealing was the most significant factor influencing the particle size. Particles with a median radius of 5–10 µm were formed following 1-4 h annealing, and the relative (%) water soluble fractions of ^{90}Sr and ^{137}Cs were 3-4 % and 5-6 %, respectively (Table 1). Particles with a median radius of 3–5 µm were formed at an annealing time of 5–21 hours, and the (%) water soluble fractions of ^{90}Sr and ^{137}Cs were 4-7 % and 6-12 %, respectively.

Table 1. Characteristics of oxidized fuel U particles prepared by annealing of original UO_2 fuel. Particle size (Rm = radius of the lognormal size distribution) and water-soluble fraction (% of ^{137}Cs or ^{90}Sr activity) are shown as a function of annealing time.

Annealing period (h)	T=400ºC		T=600ºC		T=900ºC		Water-soluble fraction (%)	
	$R_{m,\,\mu m}$	s	$R_{m,\,\mu m}$	s	$R_{m,\,\mu m}$	s	^{137}Cs	^{90}Sr
Based on sedimentation in water (Kashparov, 2009a)								
3	7.9	0.66	-	-	-	-	-	-
4	-	-	9.5	0.81	9.9	0.58	-	-
7	4.4	0.77	-	-	-	-	-	-
8	-	-	4.1	0.53	3.7	0.45	-	-
12	-	-	4.4	0.53	4.0	0.44	-	-
13	3.9	0.54	-	-	-	-	-	-
16	-	-	3.2	0.56	3.1	0.47	-	-
21	3.0	0.36	-	-	-	-	-	-
Based on imaging (Kashparov et al., 2019; Kashparov et al., 1996)								
1	6.3	0.63	-	-	-	-	6	2.9
3	4.8	0.52	-	-	-	-	5	3.9
5	3.8	0.44	-	-	-	-	6	4.0
7	3.5	0.41	-	-	-	-	9	4.6
13	3.7	0.42	-	-	-	-	10	6.2
21	3.1	0.36	-	-	-	-	12	6.6

The obtained results (Table 1) are in good agreement with the fraction of radionuclides formed by condensation in radioactive fallout (Kashparov et al., 2000b) and the determination of the composition of the fuel particles (R_m=3-10) in soils at different distances (5-30 km) and directions from the Chernobyl reactor by means of autoradiography (Bobovnikova et al., 1991).

Based on the data obtained, it is possible to estimate average parameters for the size distribution of the fuel particles, depending on the production conditions (Table 2).

Table 2. Production of U fuel particles (FP) after destruction of irradiated UO_2 nuclear fuel.

Type of FP	Annealing temperature, ºC	Annealing time, h	Median radius R_m μm	Standard deviation of the log particles radius	FP density, g cm^{-3}
UZr_xO_y	>1850	-	>10	-	-
UO_2	-	-	5	0.6	10
UO_{2+x}	400-900	1-4	5-10	0.5-0.7	8
UO_{2+x}	400-900	5-21	3-5	0.4-0.6	8

The compositions of condensation particles and various fuel particle types in areas affected by particle contamination are available (Table 3). Particle compositions along the western trace are characterized by a high fraction of UO_2 and UZr_xO_y type particles with low and very low solubility and weathering rates, respectively. This is as opposed to the northern and southern traces with high fractions of UO_{2+x} particles with relatively solubility and weathering rate.

Table 3. The fractions of ^{90}Sr associated with various types of particle fallout with respective weathering rates a_0, a_1, a_2, a_3 in areas affected by the Chernobyl accident (Kashparov et al., 2019; Kashparov, 2009a; Kashparov et al., 2000b) .

Deposition	**Global fallout, Kyshtym**	**Areas affected by the Chernobyl accident**					
		West < 20 km	**West 20-60 km**	**South < 10 km**	**South 10-50 km**	**North and East < 10 km**	**North and East 10-60 km**
Condensation water soluble form, **a_0**	1	0.02	0.05	0.03	0.05	0.03	0.05
FP of UZr_xO_y, **a_1**	0	0.18±0.05	0.05±0.02	0.07±0.03	0	0.05±0.02	0
FP of UO_2, **a_2**	0	0.5±0.2	0.55±0.2	0.19±0.15	0.20±0.15	0.2±0.1	0.2±0.1
FP of UO_{2+x}, **a_3**	0	0.3±0.2	0.35±0.2	0.71±0.15	0.75±0.15	0.72±0.1	0.75±0.1

Data summarized in Table 3 are reflected in the fraction of ^{90}Sr determined to be associated with chemically stable particles in soil samples collected from various distances and directions Figure 4.

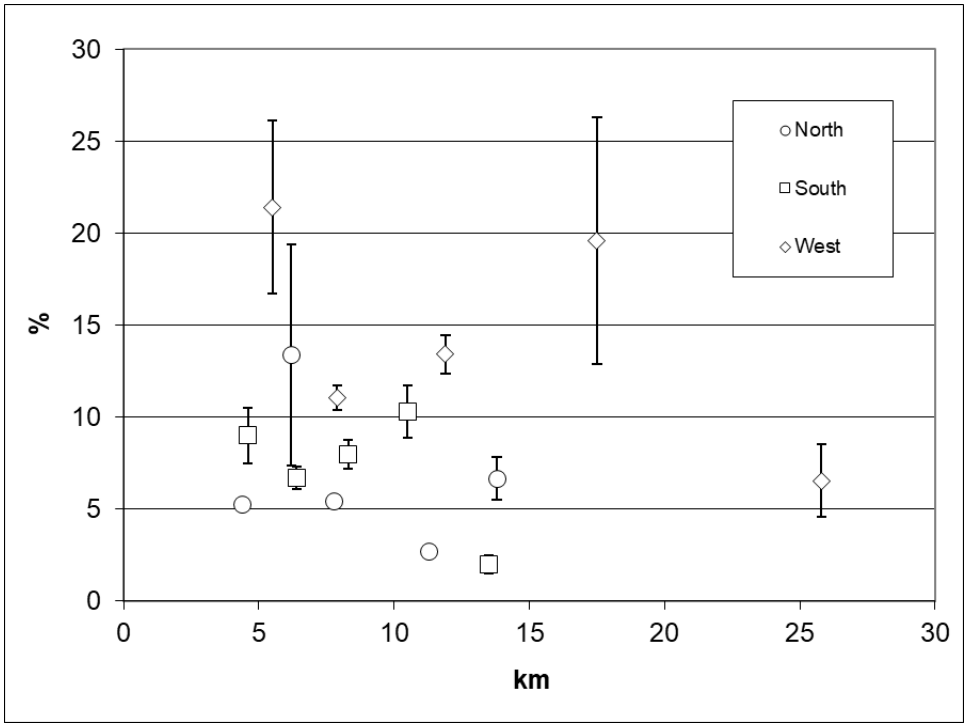

Figure 4. Fraction of ^{90}Sr in the soil associated with fuel particles of high chemical stability, plotted as a function of distance away from ChNPP (Kashparov et al., 2004b).

Parametrization of the particle weathering rates for the various fuel particle types are available as transformation constants (Table 4).

Table 4. Weathering constants (k_i, $year^{-1}$) for radioactive particles as a function of pH in the soils. The oxidation of UO_2 particles was based on annealing in air at 400ºC for a period of 1, 3, 5, 7, 13 and 21 h (Kashparov et al., 2000b).

Deposition	pH of soil solution		
	4.0	5.0	6.9
water soluble form, $\mathbf{k_0}$	∝	∝	∝
FP of U-Zr_x-O_y, $\mathbf{k_1}$	0	0	0
FP of UO_2, $\mathbf{k_2}$	0.062 ± 0.001	0.018 ± 0.001	0.012 ± 0.001
FP of UO_{2+x}, $\mathbf{k_3}$	0.79 ± 0.13	0.28 ± 0.05	0.19 ± 0.04

The parameters in the model of relevance for the behavior of radionuclides in the soil (rate constants, $\boldsymbol{n_{ij}}$) and for the root uptake by plants (concentration ratio, ***CR***) after leaching from radioactive particles (A_i). Behaviour in soil after leaching is assumed to be identical to the behavior of radionuclides in soil after their injection in water-soluble forms. Over the last 30 years, investigations have been performed with respect to the behavior of ^{90}Sr and ^{137}Cs applied in water-soluble form to important typical for

Ukrainian soil types. Values from these studies required as model parameters are given in Table 5 (Ivanov and Khomutinin, 2015):

Table 5. Model parameters appropriate to Ukraine to be used in soil-plant models.

Type of soil (FAO-UNESCO)	**Histosols**	**Podzoluvisol**	**Greyzem**	**Phaeozems**
CIS countries classification	**Peat- and Peaty-bog soils**	**Soddy-podzolic sandy soils**	**Grey forest**	**Chernozem**
Soil groups (IAEA TRS 472)	**Organic**	**Sand**	**Loam**	**Clay**
pH	3.0–5.0	3.5–6.5	4.0–6.0	5.0–8.0
Organic matter, %	≥20	0.5–3.0	2.0–6.5	3.5–10.0
Clay, %	-	<18	18–35	≥35
Sr				
n_{01}, y^{-1}	**0.2**	**0.04**	**N/A**	**N/A**
n_{10}, y^{-1}	**0.3**	**0.15**	**N/A**	**N/A**
n_{02} (for l=10 cm) , y^{-1}	**N/A**	**N/A**	**N/A**	**N/A**
n_{02} (for l=20 cm) , y^{-1}	**0.02**	**0.12±0.08**	**0.02±0.01**	**0.02±0.01**
Cs				
n_{01}, y^{-1}	**3.1**	**1.5**	**N/A**	**N/A**
n_{10}, y^{-1}	**0.08**	**0.04**	**N/A**	**N/A**
n_{02} (for l=10 cm) , y^{-1}	**N/A**	**N/A**	**N/A**	**N/A**
n_{02} (for l=20 cm) , y^{-1}	**0.03**	**0.008±0.002**	**0.007±0.003**	**0.006±0.003**

N/A – not available

3.2 Field observation data for evaluation of model output

Based on experimental work during 2013-2018, observation data (Annex, Tables S1-S8) for uptake of ^{90}Sr in wheat grains grown in the Ivankiv area just south of the Chernobyl exclusion zone and contaminated with Chernobyl fuel particles have been made available for the present work (COMET, 2017; Otreshko et al., 2014). Recent results on fuel particles dissolution in topsoil and in the Red Forest radioactive waste trench materials showed that the fraction of ^{90}Sr present as mobile species (potential bioavailable form) has reached its maximum values (Salbu et al., 2018). The dynamics of the ^{90}Sr contamination of vegetation and grain crops are determined by the kinetics of fuel particle dissolution and by the increase in mobile ^{90}Sr-species in the root-layer.

3.3 Model development and implementation

3.3.1 Methodology, technical implementation of FDMT

As described in (Brown et al., 2018), ECOSYS-87/FDMT has been incorporated within ECOLEGO by compartmentalising and structuring the system as per the original model set up (so that there are sub-models referring to for instance, 'grass extensive', 'maize', 'beet leaves' and 'leafy vegetables', 'cow' and 'lamb' etc.) and introducing the various links between compartments and equations governing each sub-system. The implementation has covered the entire suite of radionuclides and exposure pathways to humans that were included in the original ECOSYS-87 model although subsequent focus, in relation to collation of revised parameters, has been placed on the food-chain transfer components of the model relevant to this deliverable.

Default parameters are essentially those presented in the earlier version of the model [(Müller and Pröhl, 1993); (Müller et al., 2004)] with the option available to access the newly collated datasets within the CONFIDENCE project from (Brown et al., 2018). The ECOSYS-87/FDMT model within ECOLEGO can be viewed either as an interaction matrix or as a more traditional compartmental model set up (although strictly speaking the model is not a mass-balance type approach simulating flows between compartments).

Subsequent to Brown et al. (2018) work has continued on FDMT model development using ECOLEGO version 6.5.33.

An initial important structural change to the model was to differentiate between:

- Sources – essentially for defining the input source following atmospheric dispersion modelling
- Receptors – Sub-models ('blocks') incorporating units such as intensive grass-land, crop land (for given plant type) etc. receiving radionuclide deposition
- Processing and storage of different food and feedstuff – for defining parameter related to these categories
- Dose calculation – where the configuration for human dose calculations can be performed. Sub-models ('blocks') are provided as stand-alone units for human dose quantification.

In so doing, each of the abovementioned 4 generic categories (and their sub-categories) could be defined as an ECOLEGO Library item (Figure 5. New set-up in FDMT ECOLEGO using a library structure.).

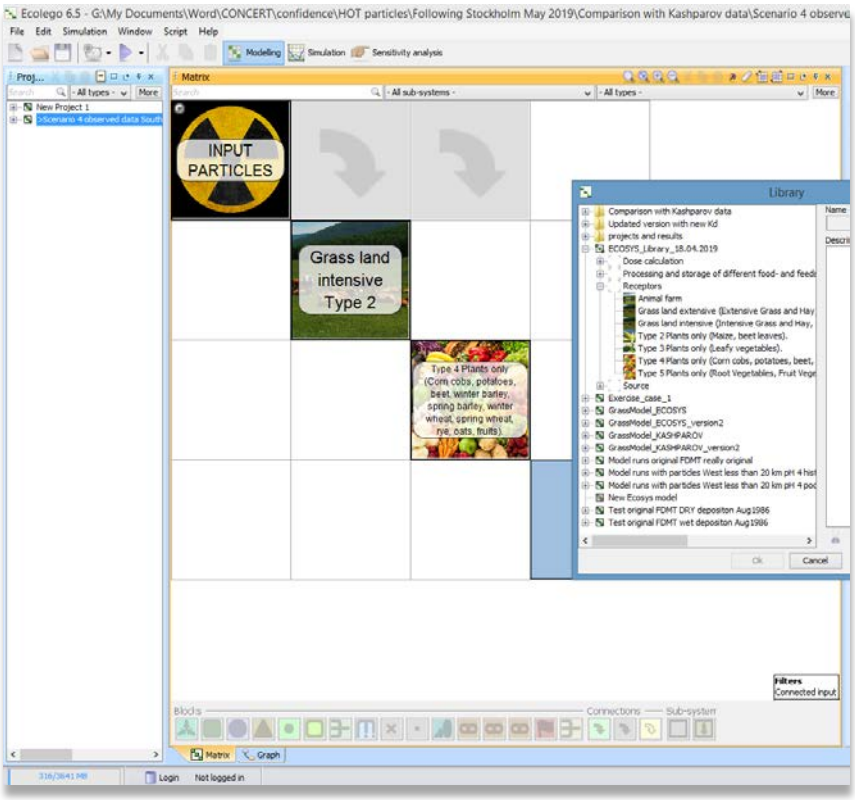

Figure 5. New set-up in FDMT ECOLEGO using a library structure.

The advantage of organizing the model in this way is that the user can select specifically what they are interested in for any given model run without invoking the entire FDMT model. For example, the assessor might be only interested in activity concentrations in a particular foodstuff, such as milk, in which case they would need only to configure a model incorporating a source, an intensive grass-land receptor and optionally a 'Processing and storage of different food- and feedstuff' block. In theory, this should provide the assessor with a means to focus their analysis by excluding extraneous information and, moreover, decreases the opportunities for introducing errors (i.e. by treating each block separately, changes can be made to individual components in the library in isolation avoiding the potential to affect the entire model detrimentally). The receptor block now included the categories:

- Animal farm
- Grass land extensive (Extensive Grass and Hay, Sheep, Goat, Lamb, Roe Deer)
- Grass land intensive (Intensive Grass and Hay, Cow)
- Type 2 Plants only (Maize, beet leaves).
- Type 3 Plants only (Leafy vegetables).
- Type 4 Plants only (Corn cobs, potatoes, beet, winter barley, spring barley, winter wheat, spring wheat, rye, oats, fruits).
- Type 5 Plants only (Root Vegetables, Fruit Vegetables, Berries).

Beyond this, structural changes have been made to the model within blocks in the library. Most importantly, for our analyses, has been the separation, within relevant receptor blocks, between plant and soil models (Figure 6). The advantage of organizing this way is simply related to flexibility, in the sense that new model components can be replaced and tested, as described below.

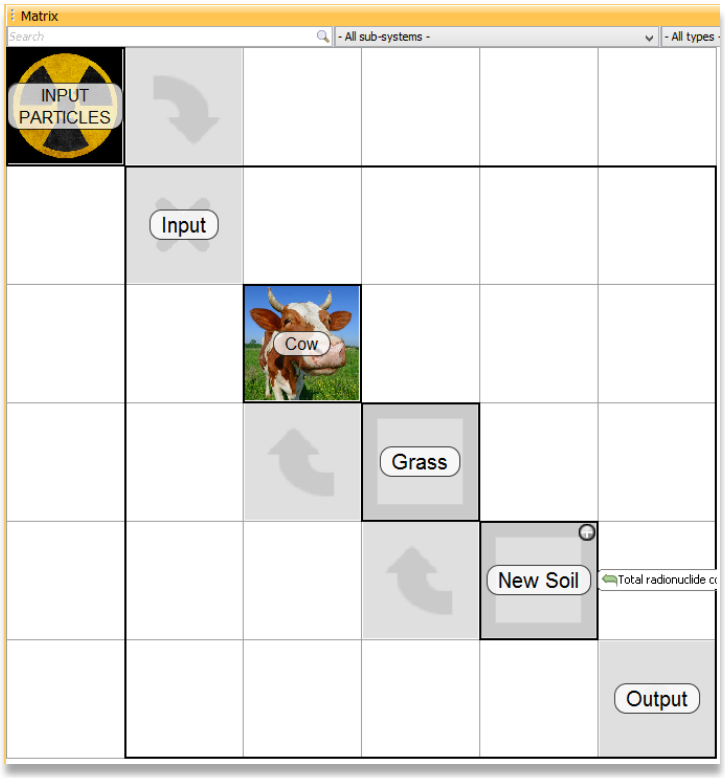

Figure 6. Interaction matrix for source and receptor block: Grass-intensive

3.3.2 The revised soil model

The new soil model, appropriate for modelling the presence of fuel particles, described earlier in this report (Section 3.1) has been set up within ECOLEGO with a minor modification to retain the process of fixation for Cs-137. With the new FDMT in ECOLEGO model structure this newly-developed soil model can be simply 'plugged in' to replace the original (FDMT) soil model. The compartmental model describing the system is provided in Figure 7.

The three compartments with the prefix FP relate to fuel particles comprising of U-Zr-Oxides, UO_2 and UO_{2+x}. Each fuel particle type will have a specific weathering rate that changes as a function of pH (as specified in Table 4, Section 4.1). Note that radioactive decay is accounted for in the new soil-particle model.

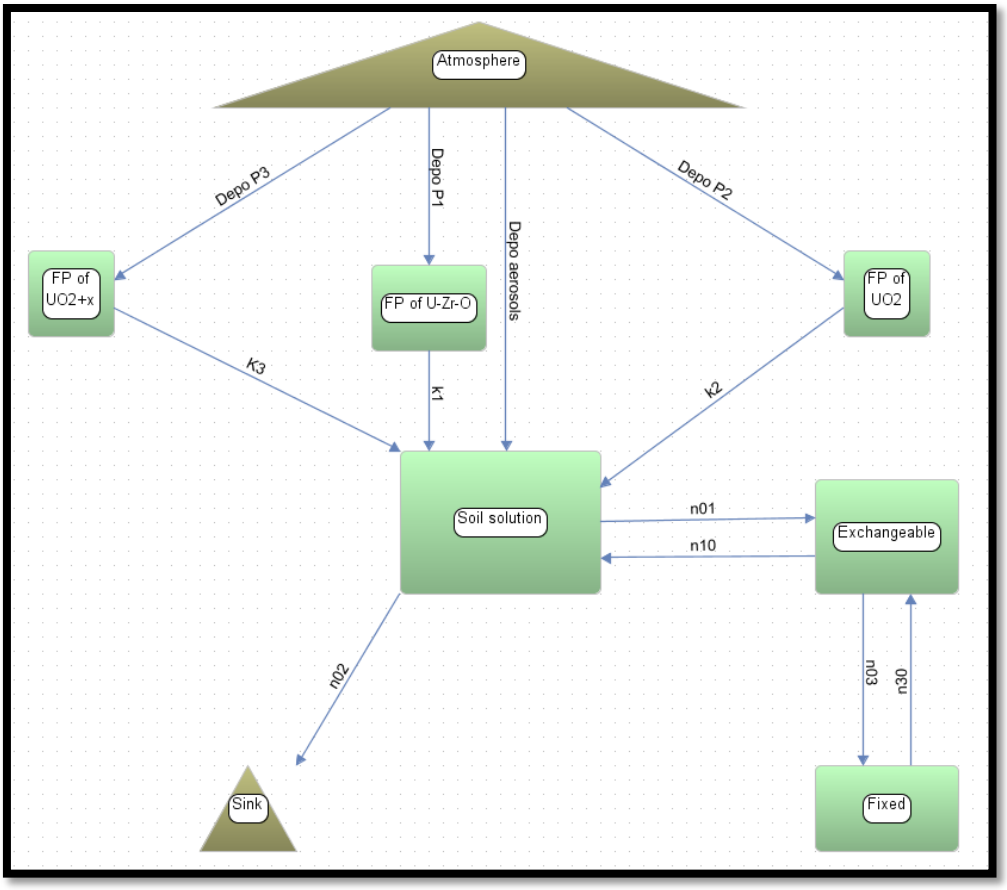

Figure 7. Graphical model depiction showing the set up for the new soil model.

Furthermore, some modification has been required to the model input. In the original version of FDMT, dry deposition is derived from the time-integrated activity concentration in air for a given radionuclide. In the new version of the model, the user defines the total deposition, the fraction of aerosol and the fractions that are allocated to dry and/or wet deposition. If there is a component of particles that is defined, by the user, as being associated with dry deposition, the modified version of the model can be used to derive integrated air concentrations (for application in other parts of the model) through dividing by a defined (maximum) deposition velocity.

In the current version of the model, there is an assumption that particles are deposited directly to soil, i.e. there is no interception by vegetation although we acknowledge in reality this will happen. The aerosol component can be modelled to follow the same pathway as aerosols in the original model set up, i.e. the component is subject to interception, translocation (i.e. uptake in the foliage and transfer to other parts of the plant) and weathering from the plant (grass or crop canopy), and will thus contributed to elevated activity concentrations on plants and within the food-chain in the first months of the accident (FDMT refers to this component as 'foliar uptake'). In contrast, the particle component of the deposition is assumed not to participate in foliar uptake and only transfer via root uptake (and resuspension[3]) can currently be considered. For the purposes of the subsequent analyses, it should be noted that the initial processes involving canopy interception have not been considered because we

[3] Note that resuspension has not been modified specifically for Ukrainian conditions and is simply incorporated as a component of the soil to plant transfer factor (in line with standard FDMT methodology), i.e. TF_soil to plant = TF_rootUptake+Enrich_factor*R_j where R_j = mass load of soil for plant 'j'.

are interested in periods that are a long time (i.e. later than the first harvest) post-accident. Thus, for our purposes, the initial conditions have been set so that the entire inventory of aerosol associated radionuclides are in soil solution.

Incidentally, it is of interest to note that FDMT essentially 'double accounts' for activity added to the system. For a given radionuclide input, a fraction of the deposited activity becomes associated with the plant canopy due to modelled interception processes but concurrently the entire deposition amount is assumed as an input directly to soil. This was organized, as such, for practical reasons (one might speculate that modelling the transfer from vegetation to soil over time via processes such as weathering using an Microsoft EXCEL™ set up would have been a non-trivial task) and, as noted by Müller et al. (2004), "*This simplification is due to the lack of experiments separating clearly between deposition on the soil and that on the overhead canopy. A slight over-prediction of the soil contamination for depositions during the vegetation period might be introduced by this assumption*."

3.3.3 Scenario description

The new model runs have been made assuming an input of 1000 Bq/m^2 of each of ^{137}Cs and ^{90}Sr into the system.' because we are only modelling times distant from deposition, this was the only input required for the scenario, irrespective of whether deposition occurred by wet or dry deposition.

Further considerations were also required with regards to soil parameters. Because we were making predictions for specific locations so that comparisons could be made with empirical data, a generic soil bulk density of 1250 kg/m^3 for a sampling depth of 0.2 m was used (Kashparov, V. pers. comm.). A generic (effective) porosity was also used, being set to 0.2 a standard value applied for these types of compartmental models [see (Dowdall et al., 2012)]. Although parameters were available for different soil types, the focus has been on podzoluvisols since these constitute the main soil category for which empirical data are available.

The simulations endpoints to be considered were: activity radionuclide concentrations in soil and in selected crops (oats, rye, wheat and barley) and bioavailable (plus reversibly-bound) fractions corresponding to the available empirical datasets. Simulation periods were up to 33 years following the deposition event, which was assumed to occur on the date of the Chernobyl reactor accident (April 26th 1986). Here simplifications were made in the sense that the deposition was modelled to occur within the course of a single day in contrast to the actual situation where deposition occurred, for any given location, sporadically over the course of the days and weeks following the Chernobyl accident (Beresford et al. 2016). This simplification of the input source term has minimal impact on subsequent predictions given the long time spans considered in this work.

Additional scenario details, including the composition of the particles (fraction of each fuel particle component) and pH are provided in Table 6.

Table 6. Details of various deposition scenarios within or in the vicinity of the Chernobyl exclusion zone.

Scenario		Direction from reactor	Deposition (fraction)				pH	Field observation data available [4]
			Condensation particles	UZr_xO_y	UO_2	UO_{2+x}		
1	Global fallout (reference), Low pH	South	1	0	0	0	4	-
2	Global fallout (reference), Medium pH	South	1	0	0	0	5	-
3	Global fallout (ref), High pH	South	1	0	0	0	6.9	-
4	Observed data, Low pH	South	0.05	0	0.20±0.15	0.75±0.15	4	Grain ^{90}Sr Bq/kg, bioavailable fraction
5	Observed data, Medium pH	South	0.05	0	0.20±0.15	0.75±0.15	5	Grain ^{90}Sr Bq/kg, bioavailable fraction
6	Observed data, High pH	South	0.05	0	0.20±0.15	0.75±0.15	6.9	Grain ^{90}Sr Bq/kg, bioavailable fraction
7	Observed data soil + grass, Low pH	West <20km	0.02	0.18±0.05	0.5±0.2	0.3±0.2	4	Grass ^{90}Sr Bq/kg, bioavailable fraction
8	Observed data soil + grass, Medium pH	West <20km	0.02	0.18±0.05	0.5±0.2	0.3±0.2	5	Grass ^{90}Sr Bq/kg, bioavailable fraction
9	Observed data soil + grass, High pH	West <20km	0.02	0.18±0.05	0.5±0.2	0.3±0.2	6.9	Grass ^{90}Sr Bq/kg, bioavailable fraction

[4] Otreshko, L.M., Levchuk, S.E., Yoshchenko, V.I., 2014. Activity concentration of ^{90}Sr in grain on fuel traces of Chernobyl radioactive fallout. Nuclear Physics and Atomic Energy 15, 171-177.

Each of the scenarios has been mapped onto a given location and year for which data have been collated (Table 6). In order to provide input to the model simulations, the measured radionuclide in soil activity concentrations have been decay corrected to the time of deposition (1986) and then converted to a contamination density (Bq m^{-2}) at time = 0, by multiplying by the bulk density, depth of rooting zone. The model was then run (forward in time from 1986) and results collated for the various time periods of interest (i.e. the years for which radionuclide in soil and grain data were available). This will lead to the prior expectation that the model will underestimate total radionuclide activity concentrations in soil because the model involves a loss from the system, due to the process of leaching to deeper soil layers, whereas the back-calculation using a physical decay correction clearly invokes a 'closed system'. However, it is generally accepted that losses of radionuclides from the rooting zones of Chernobyl exclusion zone soils have not been substantial even following several decades post-accident (Kashparov pers. comm.). This means that the comparison can at least be used to see whether the model is providing sensible results. This process of calculation may appear to suffer from being tautological, at least for the simulations made for radionuclide activity concentrations in soil, because the same dataset is being used as input to the model and subsequently as a test for model efficacy. that It should be re-emphasized that the comparison of empirical and simulated data, for soil radionuclide activity concentrations, in this way can, by no means, be used as an initial validation of the model.

Additionally to the model set-up as described above, the soil-plant model originally described by (Absalom et al., 2001), which allows predictions to be made with respect to ^{137}Cs in soil solution and grass with time (based upon soil parameters such as percentage clay and exchangeable K content), was considered as an alternative to perform simulations for the scenarios described above. It should be stated that the 'Absalom model' does not deal with particle source terms. In the Absalom model has been extended to include wheat and barley and the model restructured to test for parameter redundancy leading to the slightly modified version of the model presented by (Tarsitano et al., 2011). The mathematical specification of Absalom et al. (2001) as presented in Appendix 1 of (Tarsitano et al., 2011) is the version that has been implemented within the ECOLEGO modelling platform (after fixing some errors in Tarsitano et al.).

The 'Absalom' model has the advantage that soil type can be considered specifically and consequently as inputs it requires data on gravimetric clay content (g/g), gravimetric organic content (g/g), pH and exchangeable potassium ($cmol_c/kg$). As an adjunct to the scenario description some additional effort was placed on defining the Ukrainian podzoluvisols with respect to these parameters. Soil pH was one of the few parameters reported explicitly in the aforementioned test data sets (Table 6).

An indicative value of soil acidity, of pH 6.61, was used based on data from the site Prybirsk (with co-ordinates 51.02506; 30.05313) where wheat (Tríticum) was sampled in 2011. (Ivanov and Khomutinin, 2015) provides information on exchangeable potassium, expressed as K_2O (mg/kg), from which representative values for $[K]_{exch.}$ can be derived for podzoluvisols in contaminated areas of Ukraine. Finally, since data for site specific clay and organic data were unavailable, indicative values for podzoluvisols (in fact sampled in Poland) were used from (Vandebroek et al., 2012). The parameter defined in (Tarsitano et al., 2011) as 'a_1' (plant-dependent empirical constant) was taken as that relating specifically to wheat. These indicative input parameters are provided in Table 7, all other parameters have been left as defaults.

Table 7. Parameters used in the Absalom model set-up.

Clay gravimetric (%)	**Organic gravimetric (%)**	**$[K]_{exch}$ cmolc kg-1**	**pH**	**a_{1wheat} $log_{10}(L\ kg^{-1})$**
9.1	1.22	0.1	6.61	3.45

Clearly, much more could be done in terms of adjusting these parameters to provide an indicative range of transfer but for this initial 'scoping' analysis this selection was considered to suffice.

Other foodstuffs – food-chain soil – grass - cow milk

In order to explore the effect of using a bespoke soil radioactive particle model on the potential for radionuclide transfer to other components of the human food-chain, some additional analysis was undertaken by simulating transfer to grass and cow's milk (from cows grazing on contaminated pasture). Scenario 6 (in Table 6), was used as the base case for this and both FDMT and a variant of FDMT with the new soil (particle) model (Figure 8) were run, for ^{137}Cs only, using an input deposition to grass of 50 Bq/m^2 aerosols (equivalent to a fraction 0.05 aerosol for a total deposition of 1 kBq/m^2). Deposition was included for these simulations, but not in the cases considered earlier in the report, simply to demonstrate the importance of 'initial' post-depositional processes in determining radiocaesium activity concentrations in food-chains compared to the long-term soil-associated processes. Concurrently, a starting deposition of 1 kBq/m^2 directly to soil was modelled, this being assumed to be present in the fractions of various FPs, as specified by Scenario 6, for the new soil model runs and entirely as a homogenous input for the standard FDMT model (as this model does not differentiate between physical forms of deposited radionuclides).

Derivation of distribution coefficients and activity concentrations associated with various soil components and transfer to crops

It is useful to derive model-based distribution coefficients, K_ds, for comparison with empirical datasets and other models and set ups.

The starting point for this is to simplify the soil model system by assuming that the soil solution and 'exchangeable' (reversibly-bound) compartments reach equilibrium rapidly compared to the time periods required for substantial exchange between other compartments (e.g. by fixation and leaching from the system). This allows the two compartment system to be set up as shown in Figure 8.

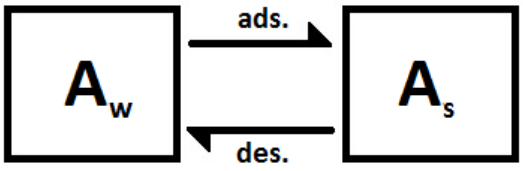

Figure 8. Simplified conceptualisation of the two-compartment system with Activity (Bq) in soil solution, A_w, Activity (Bq) in (reversibly-bound) solid phase, A_s, and the processes of adsorption and desorption.

Furthermore, we make the simplifying assumption that the activity in the 'exchangeable' compartment constitutes the activity associated with the solid component of the soil. In so doing, the following equations can be defined :

$$\frac{dA_w}{dt} = \lambda_{des.}A_s - \lambda_{sor.}A_w \quad (10)$$

Where

A_w = Activity (Bq) in water phase (soil solution)

A_s= Activity (Bq) in solid phase (exchangeable compartment)

$\lambda_{des.}$ = Rate constant for desorption (e.g. d^{-1})

$\lambda_{sor.}$ = Rate constant for adsorption (e.g. d^{-1})

At equilibrium :

$$\frac{dA_w}{dt} = \lambda_{des.}A_s - \lambda_{sor.}A_w = 0 \quad (11)$$

And thus

$$\lambda_{des.}A_s = \lambda_{sor.}A_w \quad (12)$$

In accordance with the equations provided by Fernandez et al. (2006), the relationship between activity (in a soil (or compartment) volume of 1 m^3 and thus with units of Bq m^{-3}) and activity concentration for soil solution and the soil solid fraction can be defined as :

$$A_s = C_s(1-\omega_a)\rho_s \quad (13)$$

$$A_w = C_w\omega_a S \quad (14)$$

Where

C_s = Activity concentration in soil solid (reversibly-bound) fraction (Bq/kg)

C_w = Activity concentration in soil solution (Bq/m^3)

ω_a = accessible porosity (dimensionless)

ρ_s = density of soil (kg/m^3 d.w.)

S = Saturation of soil (dimensionless and assumed to = 1, i.e. soil is saturated to maximise exchange. This term is removed from all subsequent equations)

Distribution coefficients, k_d, can be determined experimentally or theoretically from the model set up. The common definition (Fernandez et al., 2006) is :

$$k_d = \frac{C_s}{C_w} \quad (15)$$

By rearranging Equations 13 and 14 and substituting into Equation 15 we end up with

$$k_d = \frac{A_s}{(1-\omega_a)\rho_s} \cdot \frac{\omega_a}{A_w} \quad (16)$$

We can also define A_w in terms of A_s from Equation 12 and substitute this into Equation 16. Cancelling the A_s term, as it occurs in the numerator and denominator, This gives :

$$k_d = \frac{\omega_a}{(1-\omega_a)\rho_s \frac{\lambda_{des.}}{\lambda_{sor.}}} \quad (17)$$

In accordance with (Fernandez et al., 2006), the total activity concentration in soil needs to be derived as this is comprised of both the activity in solution and activity associated with the soil fraction.

$$C_{soil\_tot} = \frac{A_s + A_w}{M_s} \quad (18)$$

Where

C_{soil_tot} = Total radionuclide activity concentration in soil (Bq/kg d.w.)

M_s = Mass of soil in given volume (kg d.w.)

This equation has been modified slightly, for our purposes, to account for the activity associated with fuel particles so that:

$$C_{soil\_tot} = \frac{A_s + A_w + \sum_1^3 A_{FP}}{\rho_s \times Area \times L_{depth}} \quad (19)$$

Where : $\sum_1^3 A_{FP}$= Activity associated with the three FP components (Bq)

ρ_s = density of soil (kg/m^3 d.w.)

Area = Area over which deposition occur (1 m^2)

L_{depth} = rooting depth (m)

The activity concentrations of ^{137}Cs and ^{90}Sr in the crops : oats, rye, wheat and barley have been derived for the specific sites where data are available. These values have been derived by simply multiplying the activity concentrations in the bioavailable and reversibly-bound component of soil (in turn derived by dividing the activity in soil solution and the reversibly-bound compartment in soil by the mass of the soil compartment in a similar fashion to that shown in Equation (9) above) by the crop specific (soil to plant) concentration ratios reported in Brown et al. (2018).

The rationale for performing the derivation in this way is supported by the expectation that all activity associated with fuel particles, at any given time, will be occluded from biological interaction and should thus not be contained within the soil to plant transfer calculations. Moreover, the empirical datasets from which soil to plant concentration ratios (and as used in FDMT) have been collated are primarily based on experimental conditions, where radionuclides have been added in solution, or field conditions, under which aerosol deposition will primarily have occurred (see for example underlying datasets for Müller, H., Pröhl, G (1993) (1993)), and therefore do not represent situations where particles are present in the system with their concomitant 'occluded' fraction of activity. The use of the soil solution (bioavailable) and reversibly-bound component of radionuclides in making transfer calculations was thus a means of trying to account for this. Nonetheless, the rationale becomes weakened somewhat by the consideration that soils initially receiving aerosol associated radiocesium will with time also exhibit an occluded fraction of activity as the processes of fixation and intercalation

progress (Hird et al., 1996; Vidal et al., 1995). The insurmountable problem remains that soil to plant concentration ratios specifically collated for soils containing particles with time were not available.

Other options exist for the derivation of crop activity concentrations from the new fuel particle - soil model. Ideally, soil solution to plant concentration ratios might have been employed. In fact substantial work has been conducted on the derivation of such values as exemplified by the Absalom model considered earlier and the comprehensive studies at the University of Barcelona (e.g. Camps et al., 2004) and Katholieke Universiteit Leuven [e.g. (Smolders et al., 1997)]. From these studies a consistent observation is that the soil (solution-exchangeable) concentrations of competing ions, primarily potassium, are important factors determining radiocaesium soil to plant uptake. For strontium, calcium and magnesium concentrations have a strong influence (Camps et al., 2004). In fact, empirically-based regression equations are available to derive soil solution to plant CFs, for a limited number of plant types, for both Cs and Sr (Prorok et al., 2016)). Nonetheless, the experimental conditions under which the concomitant experiments were undertaken and from which these equations were developed were relatively short term (typically 1 to 2 years) and their compatibility with the new fuel particle soil model in making longer term prognosis, for example we are interested in decadal times scales, is therefore questionable.

Some additional modelling has been undertaken in relation to soil to crop transfer of ^{90}Sr. There is a good correlation between the aggregated transfer coefficient, T_{ag}, of ^{90}Sr in grain and the content in the soil of exchangeable calcium as noted in (IAEA, 2006) and shown in Figure 9.

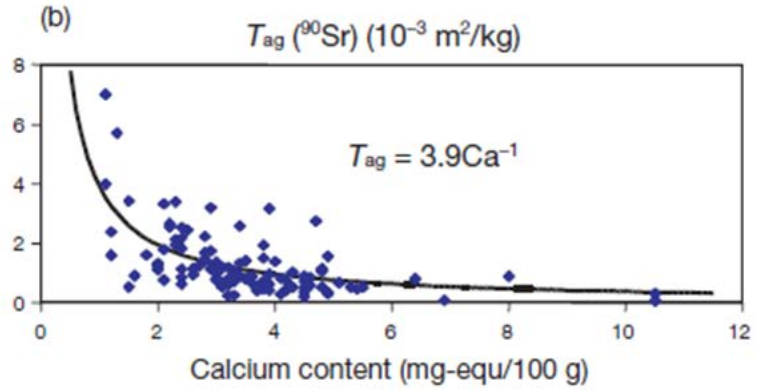

Figure 9. Transfer of ^{90}Sr into the seeds of winter rye with varying concentrations of exchangeable calcium in different soil – reproduced from IAEA (2006).

The availability of exchangeable calcium data for many of the soils for which crop transfer predictions were being derived enabled us to employ this empirical model in addition to using transfer based on the concentration ratio approach described above. For the generic case involving model-model intercomparison, an exchangeable calcium value of 2.85 mg-equ/100 g, based on the arithmetic mean of available empirical data, was used to derive a ^{90}Sr aggregated transfer factor (T_{ag}) of 1.4 x 10^{-3} m^2/kg. For the model data comparison, specific site determinations of exchangeable calcium in soil allowed bespoke ^{90}Sr T_{ag} to be derived for each measurement location.

4 Results and discussion

4.1 Kds

Soil to pore water distribution coefficients for ^{137}Cs based on empirical collations (IAEA, 2010) can be compared with values that have been calculated from the 'New' fuel-particle soil model and the Absalom model described above, respectively (Table 8). It should be noted that the derivation of the model based Podzoluvisol K_d is independent of the fuel particle composition and pH as reference to the derivation of this value (Equation 17) will testify.

Table 8. Distribution coeffcicents (K_d) for ^{137}Cs based on collated empirical data (IAEA TRS-472) and from applied models

Soil Type	**K_d L/kg**			
	Geometric Mean	***GSD***	***min***	***max***
All soils*	1.20E+03	7	4.3	3,80E+05
Sand*	5.30E+02	5.8	9.6	3,50E+04
Loam + clay*	3.70E+02	3.6	39.0	3,80E+05
Organic*	2.70E+02	6.8	4.3	9,50E+04
			Best Estimate	
Podzoluvisol - New model			7.5	
Podzoluvisol - Absalom			1.31E+04	

*IAEA TRS-472 (IAEA, 2010)

The 'New' fuel-particle soil model produces ^{137}Cs k_d values that fall at the low end whereas the Absalom model produces ^{137}Cs k_d values that fall at the high end of the empirical range for 'All soils'. In other words, the model predictions diverge to an extreme degree but both remain within what can be considered plausible. Whereas the 'New' fuel-particle soil model suggests the association of a relatively large component of ^{137}Cs activity with soil solution, the Absalom model suggests the association of a relatively large component of ^{137}Cs activity with the soil solid. The important caveat that should be added here is that the 'New' fuel-particle soil model was derived using the methodology described above (i.e. sets of equations under the section "Derivation of distribution coefficients and activity concentrations associated with various soil components and transfer to crops") and represents the relationship between activity in the reversibly bound "compartment" and the aqueous phase (i.e. the soil solution) "compartment" in soil. Essentially, we are presenting the 'steady state' k_d for a 2 compartment system, which is purely a theoretical value and is not actually used for the simulations themselves. It is helpful therefore to distinguish between these 'steady-state, theoretical' kds and the 'apparent, dynamic' k_d that could be derived from the simulation output. Alternatively, we could have calculated the ratio of activity associated with 'all solids' (including non-weathered particles) to that associated with the aqueous phase, but this was not strictly considered to be a 'steady-state,

theoretical' k_d because it is problematic to envisage how equilibration between these 'phases' could occur. The weathering of particles (and release of activity) is not, after all, a reversible reaction and the 'apparent, dynamic' k_d derived this way would have a time dependency since no equilibration could have occurred. Had we, nonetheless, used the latter method we would clearly have calculated a higher k_d at certain time points and it seems evident that further thought should be given to derivation and interpretation of this parameter within the context of particle occurrence in soil. Accepting the ^{137}Cs k_ds presented in Table 8 with the limitations as noted and ~~considering the extended period over which the simulation is being performed and~~ the observation that under normal field conditions there is often a significant decrease in the available fraction of ^{137}Cs in soils over a period of several years (Vidal et al., 1995), it seems highly unlikely that so elevated ^{137}Cs activity concentrations in soil solution, such as those inferred from the k_ds calculated for the 'New' fuel-particle soil model, could be observed. Furthermore, the current configuration of the model does not account explicitly for process of fixation for ^{137}Cs, the parameter 'n_02' or 'k_fixation' having been set to zero, and we believe that this may reduce the efficacy of the model to some degree. Having said this, the process may be partly, implicitly accounted for in the rate constant 'n_01' (in Figure 1).

In Table 9, ^{90}Sr distribution coefficients for soil and pore water have been collated for different soil types (IAEA, 2010) and compared to the model derived ^{90}Sr k_d.

Table 9. K_ds for ^{90}Sr based on collated empirical data (IAEA TRS-472) and from the applied model

Soil Type	**K_d L/kg**			
	Geometric Mean	**GSD**	**min**	**max**
all soils*	52	5.9	0.4	6.50E+03
Sand*	22	6.4	0.4	2.40E+03
loam + clay + organic*	69	5.4	2.0	6.50E+03
			Best Estimate	
Podzoluvisol - New model			7.8	

*IAEA TRS-472 (IAEA, 2010)

The model derived ^{90}Sr k_d is low compared to the geometric means of collated data for different soil types but falls well within the empirically observed ranges in values. As noted by Camps et al. (2004), K_D (Sr) can be predicted from the ratio of the Cation Exchange Capacity (CEC) vs. the sum of the concentrations of Ca and Mg in the soil solution for soils with a saturated exchange complex. For soils with an unsaturated exchange complex, the overall CEC should be substituted by the sum of exchangeable bases, i.e. the sum of exchangeable Ca, Mg, Na, K and NH_4^+ (Camps et al., 2004). Since we have limited information on soil chemistry, not least cation concentrations in soil solution, we have no possibility to explore whether the modelled k_d values provide a realistic representation of the distribution of ^{90}Sr within the soil-pore water system.

4.2 Comparison of model outputs for soil based on scenarios with and without particles

A comparison of results from two models (i.e. 'New' fuel-particle soil model and FDMT) simulations are shown in Figure 10 for Scenario 6. This scenario was selected because the pH was most similar to many of empirical datasets compiled for model comparison.

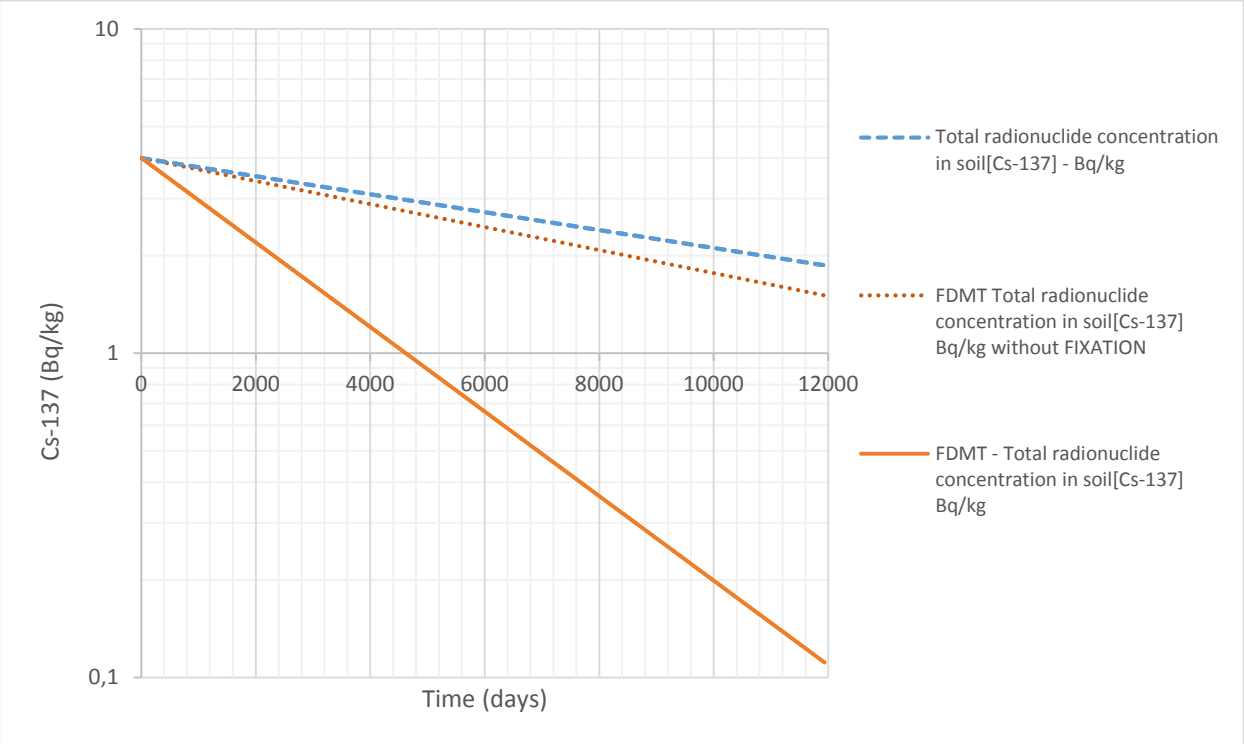

Figure 10. Activity concentrations of ^{137}Cs (Bq/kg) in soil with time (days) simulated using two models : 'New' fuel-particle soil model (dashed blue line) and FDMT (solid orange line); for Scenario 6 (South, high pH). Deposition = 1 kBq/m^2 ^{137}Cs. The dotted orange line denotes ^{137}Cs activity concentrations (Bq/kg) in soil based on FDMT without fixation.

Both simulations start with an activity concentration of ^{137}Cs in soil of 4 Bq/kg (which correspond to a deposition of 1 kBq/m^2 distributed over a soil rooting zone of 0.2 m with a bulk density of 1250 kg/m^3). It is clear that the models provide quite divergent ^{137}Cs activity concentration temporal profiles. At the end of the simulation period (ca. 12000 days), the level of ^{137}Cs predicted using the 'New' fuel-particle soil model is 17 times greater than the prediction made using the FDMT model (cf. ca 1.9 Bq/kg predicted using the former with ca. 0.11 Bq/kg predicted using the latter). The 'New' fuel-particle soil model appears to predict very little loss of ^{137}Cs from the top 20 cm of soil, most of the observed decrease in levels being attributable to radioactive decay whereas the FDMT model appears to predict considerable losses. Further inspection suggests that a large fraction of these 'losses' for the FDMT model are attributable to the process of fixation. Strictly speaking, this component of ^{137}Cs activity is not lost from the system but is retained in the surface soil in an occluded form. Setting the fixation rate to zero produces a temporal profile for the FDMT model that is quite similar to the new model (Figure 10**)**. Nonetheless, the presentation of the ^{137}Cs results from the FDMT model including fixation remains more valid (than results without fixation) because these soil activity concentrations are the ones used in subsequent calculations of activity concentrations in crops. Similar arguments could have been made to recommend presenting simulation results from the new radioactive particle model in a form

compatible with subsequent crop transfer determinations but, as will be shown later, for cases where the proportion of FP $UZrO_x$ and UO_2 are not high, the difference between total and transfer-relevant ^{137}Cs activity concentrations will not be substantial. With regard to predicting ^{137}Cs activity concentrations, the 'New' fuel-particle model, at least for this specific scenario parameterized for podzoluvisols near to Chernobyl, is more consistent, than FDMT, with the putative behavior of ^{137}Cs in soil at protracted periods post-accident.

A similar comparison has been made for ^{90}Sr as shown in Figure 11.

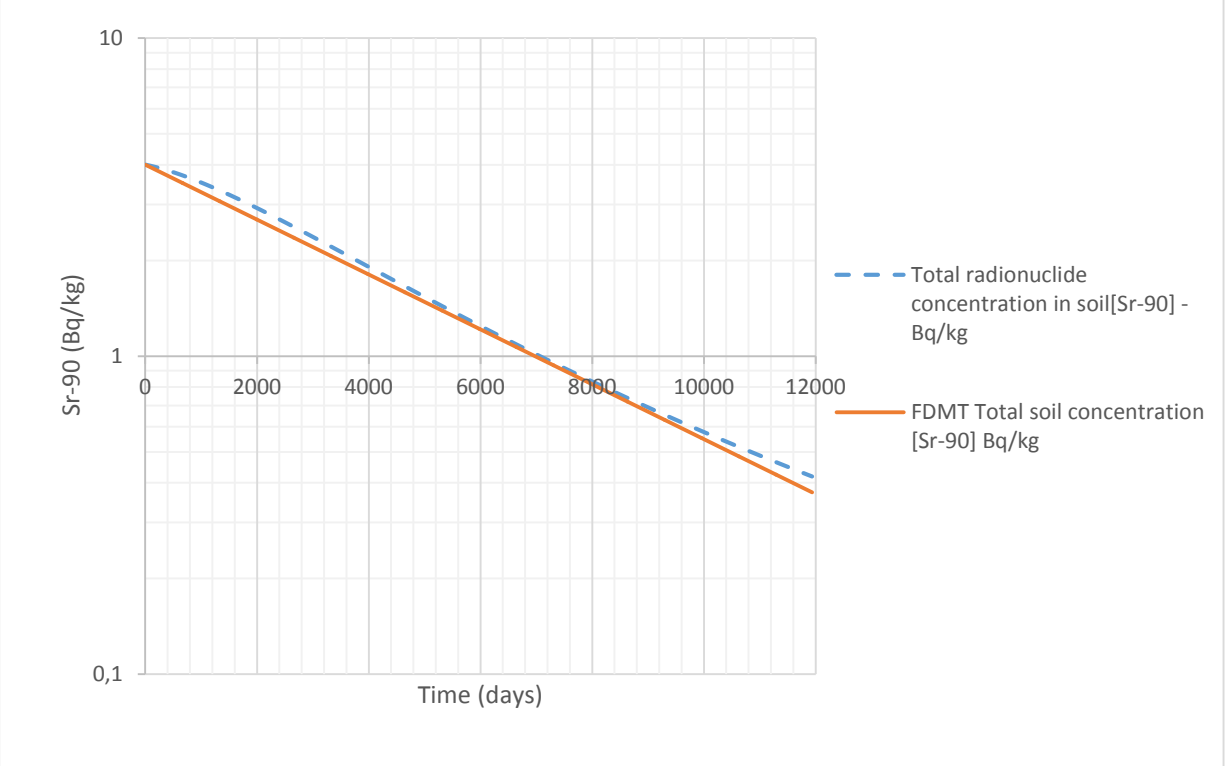

Figure 11. Activity concentrations of ^{90}Sr (Bq/kg) in soil with time (days) simulated using 2 models: 'New' fuel-particle soil model (dashed blue line) and FDMT (solid orange line); for Scenario 6 (South, high pH). Deposition = 1 kBq/m^2 ^{90}Sr.

The model simulations produce similar results throughout the analysis period. This is somewhat contrary to expectation in the sense that it is surprising that the original soil model in FDMT so closely mimics the behaviour of ^{90}Sr in soil simulated using a bespoke soil model that explicitly accounts for FP weathering. The result is quite likely to be simply coincidental, despite the suspicion that some parameterisation of the FDMT soil model could have been based on some soils that actually contained particles. As noted in Muller et al. (2004), the FDMT soil model has been modified '*according to a suggestion of (Fesenko et al., 1998) in order to allow a better adaptation to the conditions of Russia and other East European regions*.' Overall losses from the soil system (20 cm of top soil) are similar irrespective of whether this is modelled using a simple analytical approach (for 2 compartments) and leaching rate (FDMT uses a value of 3.8 x 10^{-5} d^{-1} plus a fixation rate of 9x10^{-5} d^{-1}) or a multi-compartmental set up with a different leaching rate (the new particle-soil model uses a substantially higher value of 3.3 x 10^{-4} d^{-1}) at least for the given case (podzoluvisol with an FP composition high pH as defined for scenario 6).

It is notable that the soil type specific leaching rates that have been used for podzoluvisols in the new particle-soil model are seen to be relatively high, as noted above they are in fact an order of magnitude greater than those used as default in the FDMT model. Furthermore, as considered from the perspective of the mismatch of total ^{90}Sr activity concentrations in soil between (the new particle-soil) modelled and empirical data (from the underlying datasets referred to in Table 6), the simulated downwards soil migration may not be as great as the model default leaching rates infer. Further, consideration of the new particle-soil model may be warranted through review and optimization of the parameter dictating losses from the soil system.

4.3 Influence of pH on output of new fuel-particle soil model

Simulations showing the activity concentration of ^{137}Cs with time associated with 'soil solution and reversibly-bound' component of soil for different pHs is presented in Figure 12.

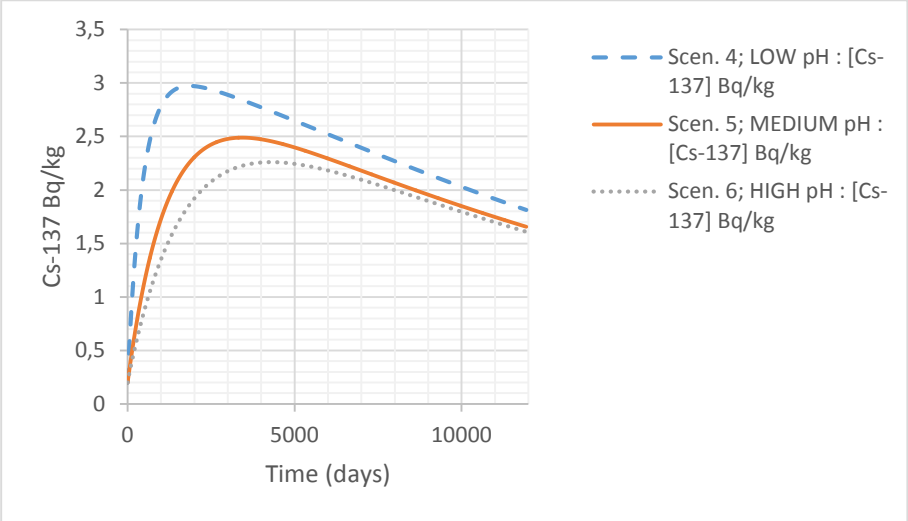

Figure 12. Activity concentrations of ^{137}Cs (Bq/kg) in the 'soil solution and reversibly-bound' component of soil with time (days) simulated using 'New' fuel-particle soil model for different pH regimes and scenarios 4 to 6. Soil type = podzoluvisols and deposition = 1 kBq/m^2 ^{137}Cs.

For the low pH scenario, a more rapid weathering and concomitant release of ^{137}Cs from particles into soil solution and the reversibly-bound compartments in soil is evident. Comparison with total ^{137}Cs activity concentrations in soil (Figure 13), for Scenario 6, high pH, suggests that a small proportion of the ^{137}Cs (3 % at end of simulation) is present in a nominally bioavailable form (corresponding to the soil solution compartment) as predicted by the model. Although a direct comparison with other studies is confounded by differences in the timing and locations from which samples were taken and the definition of what constitutes any given geochemical phase (extraction procedures are operationally defined), this value is congruent with field-based determinations of ^{137}Cs in exchangeable form for Chernobyl contaminated soils (e.g. Hou et al. (2003); Riise et al. (1990); Oughton et al. (1992)). For example, Riise et al. (1990) reported that less than 10% of ^{137}Cs was easily leachable. At low pH, bioavailable ^{137}Cs activity concentrations in soil are simulated to remain elevated compared to corresponding geochemical fractions in soil under higher pH conditions throughout the entire simulation period.

Simulations showing the activity concentration of ^{90}Sr with time associated with 'soil solution and reversibly-bound' component of soil for different pHs is presented in Figure 13:

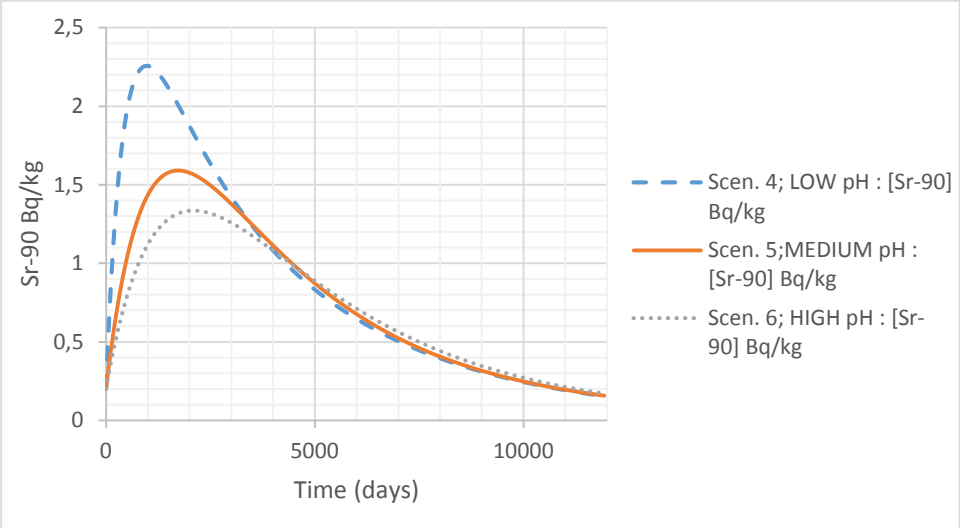

Figure 13. Activity concentrations of ^{90}Sr (Bq/kg) in the 'soil solution and reversibly-bound' component of soil with time (days) simulated using 'New' fuel-particle soil model for different pH regimes and scenarios 4 to 6. Soil type = podzoluvisols and deposition = 1 kBq/m^2 ^{90}Sr.

At low pH, 'soil solution and reversibly-bound' ^{90}Sr activity concentrations in soil are simulated to remain elevated compared to corresponding geochemical fractions in soil under higher pH conditions during the initial stages of the simulation. In fact, the ^{90}Sr levels for the low pH conditions are approximately a factor of 2 greater than for the high pH conditions when t = 1000 days. At later time points and certainly towards the end of the simulation period the activity associated with soil solution and exchangeable phases is virtually the same irrespective of pH.

For Scenario 6, high pH, the fraction of ^{90}Sr associated with the soil solution compartment is 26 % falling at a rate substantially higher than the corresponding value determined for ^{137}Cs. This again, is reasonably consistent with some field-based observations. For example, whereas up to 70% ^{90}Sr was found in the easily extractable fractions for Norwegian and Belarussian soils contaminated following the Chernobyl accident (Oughton et al., 1992), the percentage of ^{90}Sr associated with this fraction was significantly lower in the soils collected from the Chernobyl area (Oughton et al., 1992). Conversely, the modelling result corresponds less convincingly to observations made elsewhere – subsequent to leaching from FP, about 85% of ^{90}Sr has been reported to exist in solution and exchangeable forms for soddy-podzolic sandy and sandy soils in and near the Chernobyl Exclusion Zone (Kashparov, pers. comm.)

4.4 Influence of particle composition on output of new fuel-particle soil model

A comparison of results for ^{137}Cs versus time in the 'soil solution and reversibly-bound' fraction in soil between model simulations for three scenarios, corresponding to cases where all parameters have been held the same apart from fuel particle composition, are given in Figure 14.

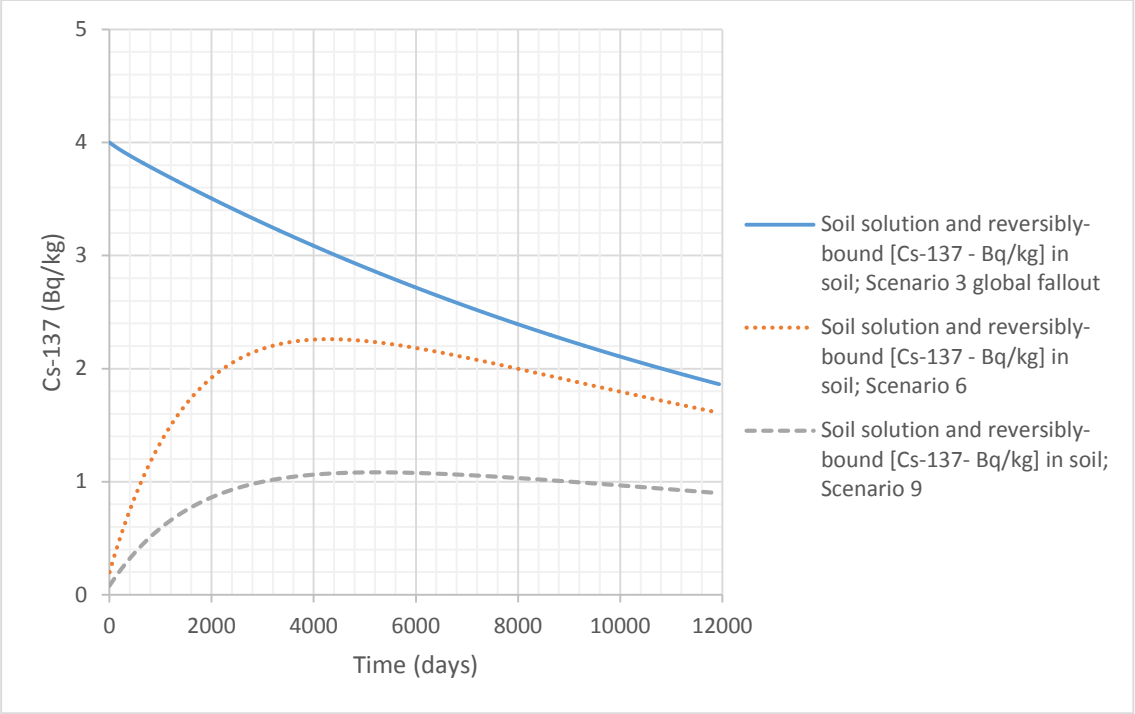

Figure 14. Activity concentrations of ^{137}Cs (Bq/kg) in the 'soil solution and reversibly-bound' component of soil with time (days) simulated using 'New' fuel-particle soil model for different FP compositions. Soil type = podzoluvisols, pH = high and deposition = 1 kBq/m^2 ^{137}Cs.

The profiles for scenario 3, which pertains to 'global fallout' with 100 % aerosol deposition, produces the same results as simulations with scenarios 1 and 2 because only pH is changed between these scenarios and this parameter solely affects FP weathering rates, which are not, by definition, present in these cases. Incidentally, it is of interest to note that should the total ^{137}Cs activity concentration in soil have been reported, which includes the radionuclide fractions associated with FPs, all time profiles would have been virtually identical following the form delineated by scenario 3 in Figure 14. This may appear to be counterintuitive in the sense that particle composition seems to have no effect on total ^{137}Cs activity concentration in surface soil until it is realised that losses from the system only occur via the soil solution compartment and leaching rates are relatively low. The model simulations show that almost all activity is retained in the top 20 cm of soil irrespective of the composition but, of course, the distribution of activity between components within the soil over time will be very different depending upon the initial FP constitution. This is illustrated in Figure 14, where the ^{137}Cs activity concentrations associated with the 'soil solution and reversibly-bound' for scenario 9 are substantially lower than the corresponding fraction for scenarios 3 and 6. This reflects the fact that scenario 9 has a substantial fraction (18%) of activity continually associated with highly recalcitrant UZr_xO_y, whereas the other scenarios do not, scenario 9 also has a relatively large fraction (50%) associated with UO_2, which exhibits a relatively low weathering rate compared to UO_{2+x} (cf. scenario 6 which has 75 % of activity in the form of UO_{2+x}). A final point to note is the temporal form of the profiles. Whereas scenarios 6 and 9 show a gradual increase in ^{137}Cs activity concentrations in the soil solution and reversibly bound fractions for the initial period, as FPs are subject to weathering and release their inventories, attaining only maximum levels once several thousand days have elapsed, the scenario involving aerosol deposition exhibits a monotonous and gradual decrease for the corresponding soil fraction.

Nonetheless, the aerosol deposition scenario retains the highest ^{137}Cs activity concentrations in soil solution and reversibly bound fractions throughout the entire simulation period.

A comparison of results for ^{90}Sr versus time in the 'soil solution and reversibly-bound' fraction in soil between model simulations for 3 scenarios, corresponding to cases where all parameters have been held the same apart from fuel particle composition, are given in Figure 15.

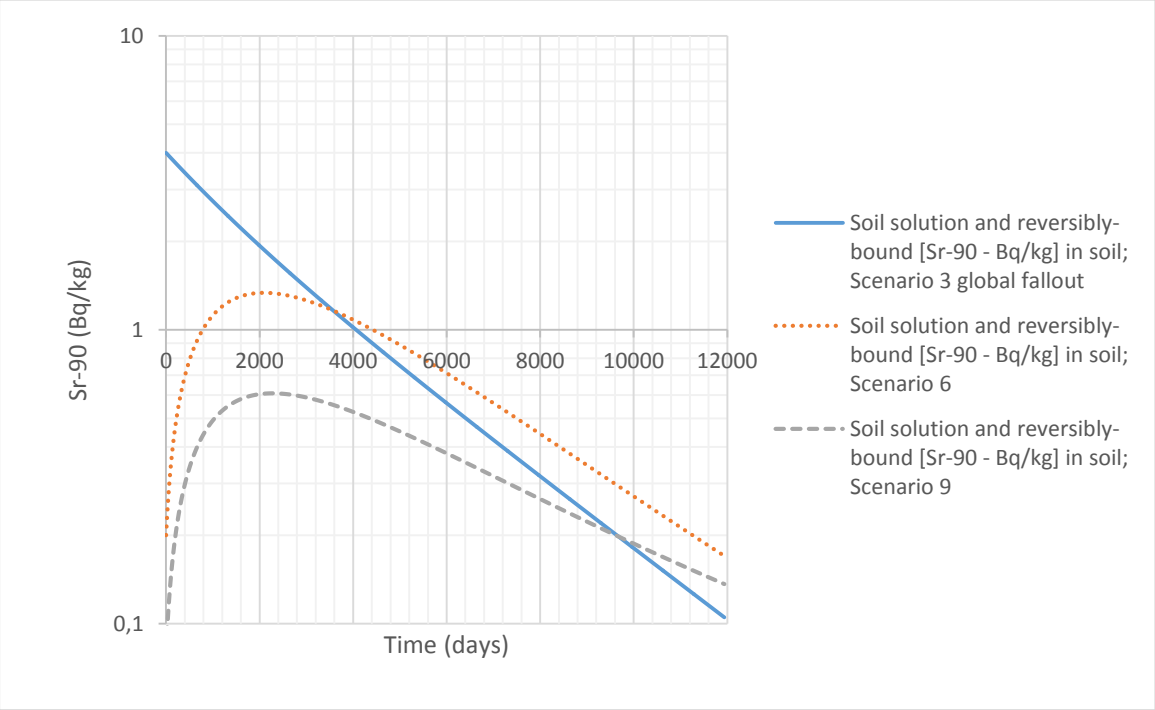

Figure 15. Activity concentrations of ^{90}Sr (Bq/kg) in the 'soil solution and reversibly-bound' component of soil with time (days) simulated using 'New' fuel-particle soil model for different FP compositions. Soil type = podzoluvisols, pH = high and deposition = 1 kBq/m^2 ^{90}Sr.

There are similarities between the temporal evolution of ^{90}Sr activity concentrations (in soil solution and the reversibly-bound component of soil) when considered as a function of scenario, and the corresponding patterns observed for ^{137}Cs. For example, the scenario involving aerosol deposition exhibits a monotonous and gradual decrease in ^{90}Sr activity concentrations in the soil solution and reversibly bound fractions over the entire simulation period whereas scenarios 6 and 9 show a gradual increase for the initial period, attaining only maximum levels (for the corresponding soil fraction) once several thousand days have elapsed, before subsequently decreasing gradually.

In contrast to the ^{137}Cs temporal profiles, the aerosol deposition scenario does not exhibit the highest ^{90}Sr activity concentrations in soil solution and reversibly bound fractions over the entire simulation period, although levels for the aerosol deposition scenario are highest in the initial period. Furthermore, the timing for when ^{90}Sr levels in soil components for scenarios involving FP deposition exceed those for aerosol deposition. For Scenario 6, where the proportion of weatherable forms of FP are relatively high, ^{90}Sr soil component activity concentrations exceed those in the aerosol deposition scenario by ca. 3500 days. A similar intersection point beyond which ^{90}Sr levels for Scenario 9 (for which refractory forms of FP dominate), are elevated above those for the aerosol deposition scenario does not occur before almost 10000 days of elapsed time.

4.5 Modelled radionuclide activity concentrations in crops

A comparison of model outputs with respect to ^{137}Cs (Bq/kg) activity concentrations in wheat are shown in Figure 16. To keep the model set up conditions similar, the high pH scenario 6 was used for the 'New' fuel-particle soil model and a 'representative' pH of 6.61 for a sampling site in Prybirsk from 2011 was arbitrarily selected for the Absalom model runs (other set-up parameters having been described earlier for podzoluvisols). Soil conditions do not affect the basic FDMT model output for activity concentrations in wheat assuming one resorts to using a generic (as oppose to soil-specific) soil to plant concentration ratio for wheat.

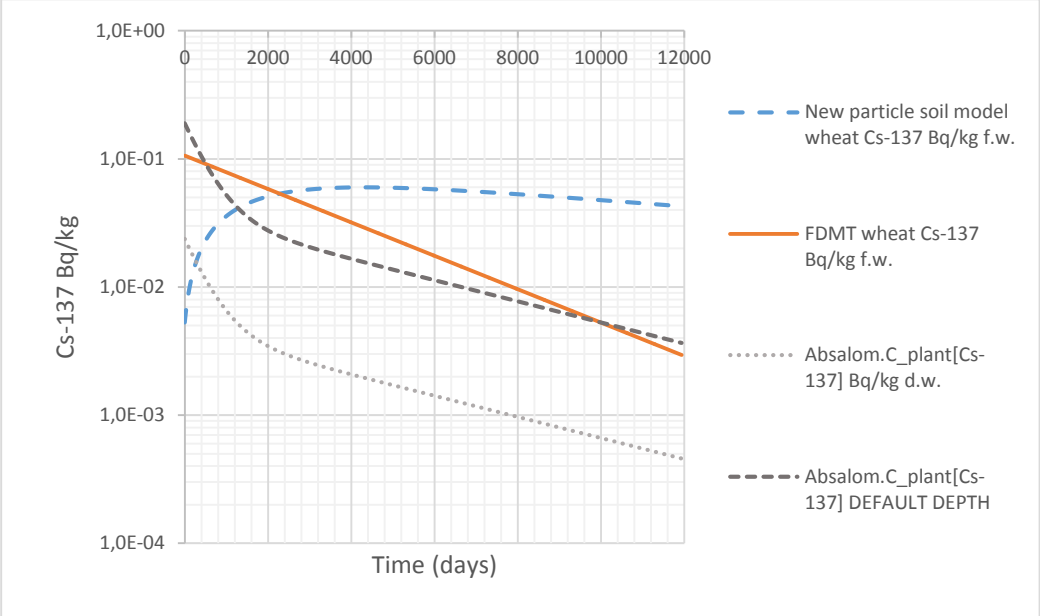

Figure 16. Activity concentrations of ^{137}Cs (Bq/kg) in wheat simulated using 3 models : 'New' fuel-particle soil model (dashed blue line), Absalom (grey dotted line) and FDMT (solid orange line); for Scenario 6 (South, high pH). Deposition = 1 kBq/m^2 ^{137}Cs. The dark grey, short-dashed line shows the Absalom model output using a default depth (over which ^{137}Cs is assumed to be distributed) of 2.5 cm.

The model outputs are very dissimilar. Whereas both FDMT and the Absalom models predict a continual decline in the levels of ^{137}Cs in wheat following the deposition event, the 'New' fuel-particle soil model does not attain maximum values before 4000 days of elapsed time. At the end of the simulation period the activity concentration of ^{137}Cs in wheat as predicted using the 'New' fuel-particle soil model is almost 2 orders of magnitude greater than that predicted using the Absalom model and ca. 15 times greater than that predicted using FDMT. The original model intercomparison was made by setting all parameters where commonality was evident to the same values. So, for the derivation of the initial activity concentration in soil a depth of 0.2 m (in line with the default specified in the new soil model) was used for all models. This approach required substantial adjustment of the deltaZ (m) parameter (defining the depth over which ^{137}Cs is assumed to be distributed) in the Absalom model from the default of 0.025 m used by the original authors. Reverting to this Absalom model default value yields results much more in line with values generated using the FDMT model. The Absalom model returns the most elevated ^{137}Cs activity concentration in wheat for the first 500 or so days using this default configuration.

The Absalom model predicts activity concentrations on a dry weight mass basis whereas the other models make predictions for fresh mass. No attempt has been made to adjust for this, although the dry matter content of wheat grain is known to be high with a value of 88 % being provided in IAEA (2010). In other words, accounting for a fresh to dry matter conversion for wheat grain would make little difference.

A comparison of model outputs with respect to ^{90}Sr (Bq/kg) activity concentrations in wheat are shown in Figure 17. As for the model simulations involving ^{137}Cs, the high pH scenario 6 was used for the 'New' fuel-particle soil model. Two variants of the approach used to determine soil to crop transfer were adopted using output from the 'New' fuel-particle soil model. The default variant used a CR value whereas 'Alternative' model employed a regression T_{ag} model based on exchangeable calcium as described in the methodology.

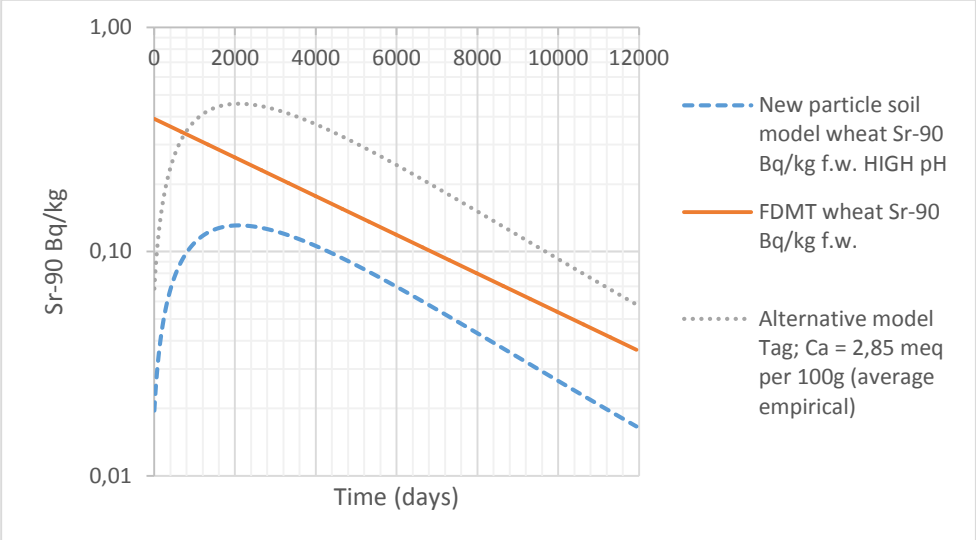

Figure 17. Activity concentrations of ^{90}Sr (Bq/kg) in wheat simulated using 3 models : 'New' fuel-particle soil model (with soil to plant CR - dashed blue line), FDMT (solid orange line) and 'Alternative' T_{ag}- regression model based on exchangeable [Ca] to calculate crop transfer from New fuel particle soil model (grey, dotted line) ; for Scenario 6 (South, high pH). Deposition = 1 kBq/m^2 ^{90}Sr.

The FDMT model can be used to predict a ^{90}Sr activity concentration in wheat that is approximately a factor of two greater than the prediction for the same endpoint that can be derived using the new particle-soil model with CR at the end of the simulation period (Figure 17). If the 'alternative' Tag based soil to plant transfer model is used (in tandem with the 'New' fuel-particle soil model), the predicted activity concentrations in the crop become substantially greater, with ^{90}Sr activity concentrations falling approximately 1.6 times above the corresponding FDMT values at the end of the simulation period. Whereas calculation from the FDMT model illustrate monotonously declining ^{90}Sr level in wheat following the initial deposition event, the predictions using both variants of the new particle-soil model (CR and Tag-[Ca] based) suggest an increase in transfer over the initial period, with a maximum occurring 5 to 6 years post deposition, followed by a similar rate of decrease, to that seen for the FDMT model, thereafter. Such a delay in transfer is in agreement with time series for concentration ratio of ^{90}Sr in grain and in 20-cm arable topsoil, which showed that a maximum uptake was reached about 30 years after the accident in the Ivankiv area south of the Chernobyl exclusion zone (Kashparov et al., 2019).

There appears to be little to be gained in replacing the ^{90}Sr soil model by a new particle-soil and CR-coupled model in its current configuration because the uncertainties involved in the model outputs (i.e. aggregated uncertainties) may be considered substantial in which case the tendency might be to adhere to the more conservative approach (i.e. retain the FDMT model). On the other hand, the new particle-soil and Tag-[Ca] based model produces the most conservative estimates of ^{90}Sr in crops between all the models for a large proportion of the simulation period (for all time points post approx. 800 days) and, by the same argument, this model might be considered as a viable replacement for FDMT. Nonetheless, concerns over the quantification of some parameters, most notably leaching/migrations rates as discussed below, may moderate this consideration.

4.6 Comparison of model output with empirical data

For comparison, predicted ^{137}Cs activity concentrations using the new particle-soil model (combined with a crop-specific CR to calculate soil to crop transfer) and measured ^{137}Cs activity concentrations in crops sampled in the Ukrainian sector of the Chernobyl exclusion zone (Annex, Tables S1-S8), are plotted in Figure 18.

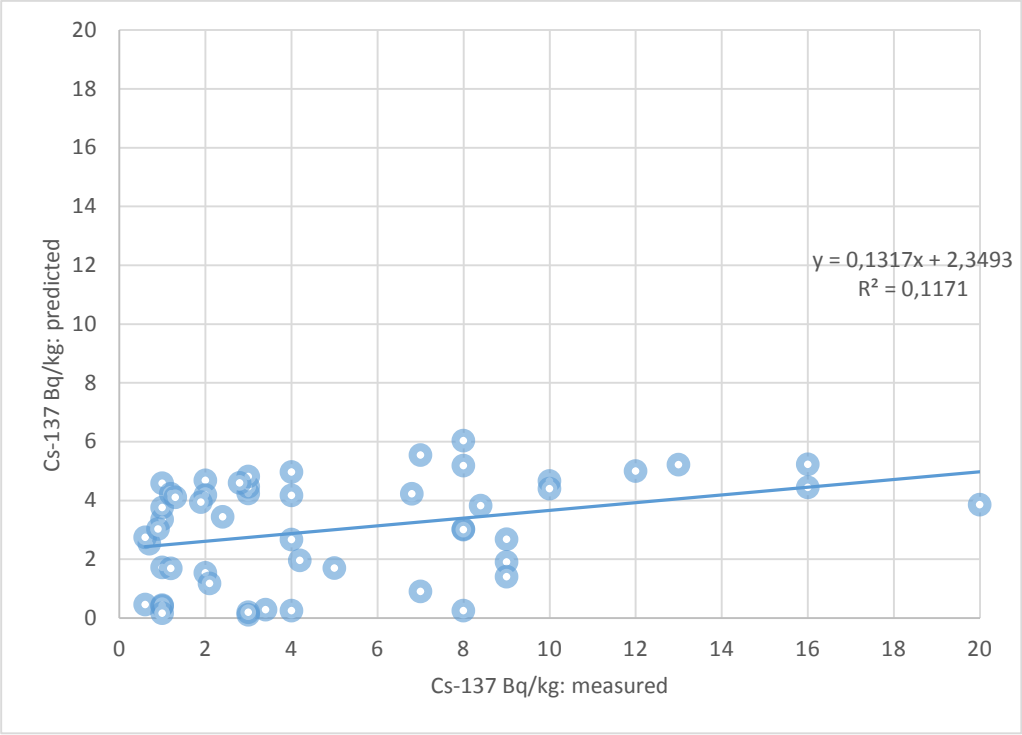

Figure 18. Activity concentrations of ^{137}Cs (Bq/kg) in crops (wheat, Rye, barley); x-axis = measured (grain data 2011-2018) and y-axis = predicted using the new particle-soil model (combined with a crop-specific CR to calculate soil to crop transfer) for the corresponding scenario and year.

The new particle-soil model (using a CR) somewhat under-predicts ^{137}Cs activity concentrations in grain, although simulated values are of the same order of magnitude as empirical determinations. By contrast, the corresponding simulations for ^{137}Cs activity concentrations in grain from the FDMT and Absalom models (albeit, for the latter, using distribution depth of 0.2 as oppose to a default of 0.025 m) result in values that are lower than empirical determinations by approximately a factor of 10 and 100 x respectively. Despite the similarity in the general magnitude of results from the new particle-soil

model with measured data, the correlation between predicted and empirical values is, in fact, quite poor.

A comparisons between predicted ^{90}Sr activity concentrations using the new particle-soil model (combined with a Tag-[Ca] approach based on site specific [Ca] determinations to calculate soil to crop transfer) and measured ^{90}Sr activity concentrations in crops sampled in or in the vicinity of the Ukrainian sector of the Chernobyl exclusion zone (Annex, Tables S1-S8)), are illustrated in Figure 20.

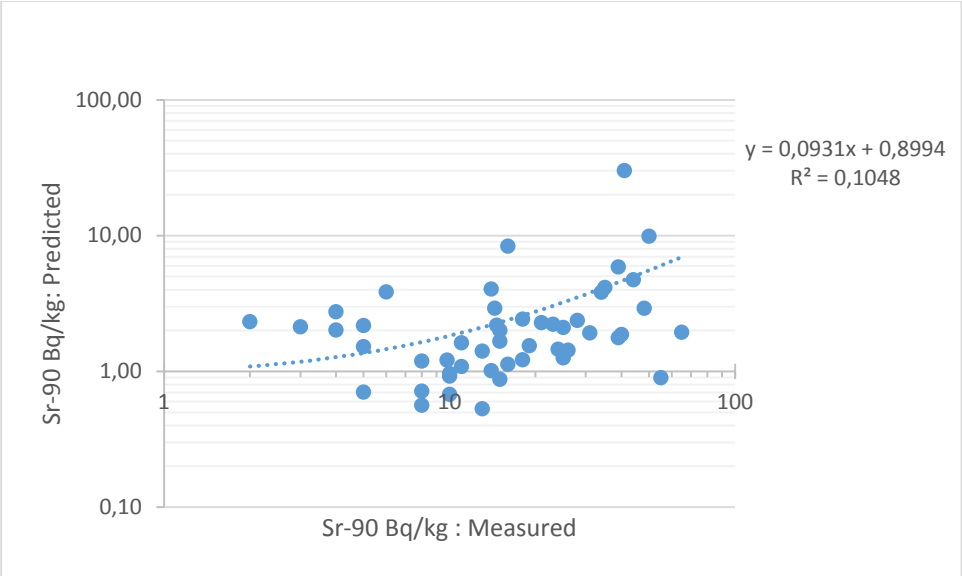

Figure 19. Activity concentrations of ^{90}Sr (Bq/kg) in crops (wheat, Rye, barley); x-axis = measured (grain data 2011-2018 as referred to in Section Table 6and y-axis = predicted (corresponding scenario and year). Note, predicted includes the use of a Tag derived from exchangeable calcium as noted in the text.

Although model simulation results for ^{90}Sr in grain are roughly of a similar order of magnitude to field-based empirical data, the correlation between predicted and measured values is poor. The model underpredicts ^{90}Sr activity concentrations in grain, in a substantial number of cases by a considerable (> 10 times) margin.

4.7 Modelling of transfer to other foodstuffs (food-chain soil – grass - cow milk)

The results from the model simulations for the soil – grass - cow milk system (the specific scenario for which is described in Section 4.3.3) are shown in Figures 20-21.

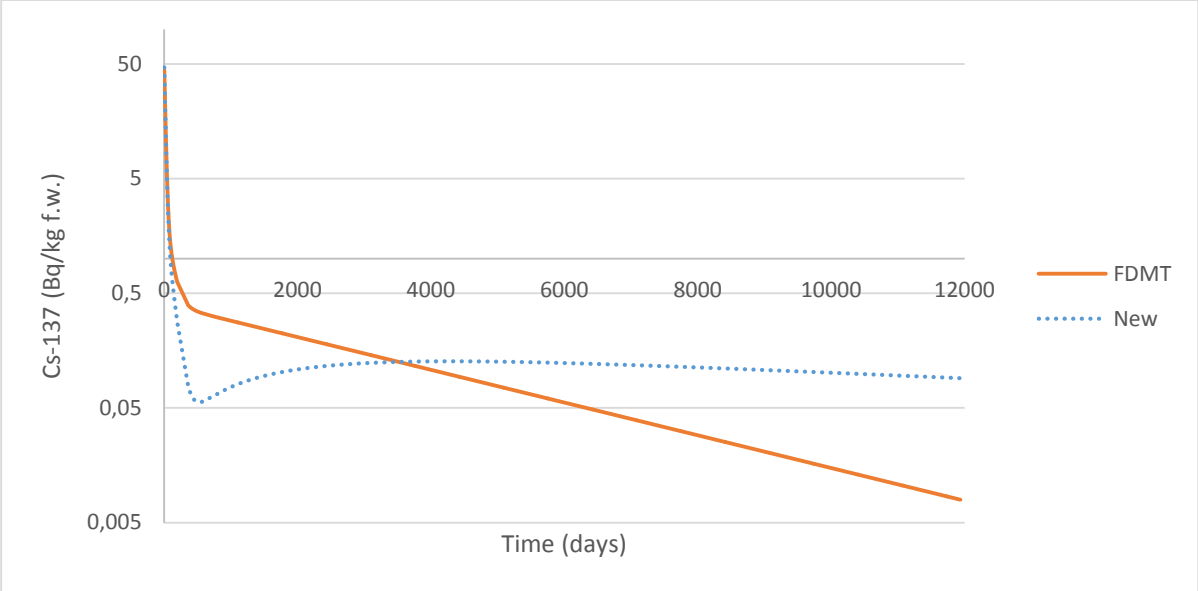

Figure 20. Activity concentrations of ^{137}Cs (Bq/kg f.w.) in grass with time (days) simulated using 2 models : 'New' fuel-particle soil model (dashed blue line) and FDMT (solid orange line); for Scenario 6 (South, high pH). Deposition ^{137}Cs = 1 kBq/m^2 to soil, 50 kBq/m^2 to vegetation.

The ^{137}Cs activity concentrations in grass (Figure 20) for both models trace an identical temporal trajectory in the initial period (up to 50 days) reflecting the predominance of processes related to radionuclide interception by vegetation shortly following deposition. At later stages, and certainly post 100 days following the deposition event, the temporal profiles diverge substantially. Whereas ^{137}Cs activity concentrations in grass using the new FP soil model fall relatively quickly before increasing gradually post 500 days, the corresponding values from the FDMT model decrease continually falling substantially below the new model outputs when time passes several thousand days.

The temporal profiles of ^{137}Cs in milk from the two models (Figure 21) exhibit similarities to the simulation outputs for grass in the sense that the temporal trajectories for both models are identical in the initial 50-day period. However, differences exist in the observation that maximum levels for milk are not observed at the time of deposition as they are for grass but attain a maximum just before 20 days of elapsed time. The temporal profiles for the two models are more complex than those seen for grass (reflecting, among other things the changing diet of cows throughout any given year) with some deviation occurring after 50 days before temporarily, in the period 200 to 400 days converging, and thereafter diverging more conspicuously. Towards the end of the simulation period, after approximately 4000 days, the ^{137}Cs activity concentrations in milk predicted using the new FP model are substantially greater (i.e. by up to a factor of 10) than those predicted using FDMT.

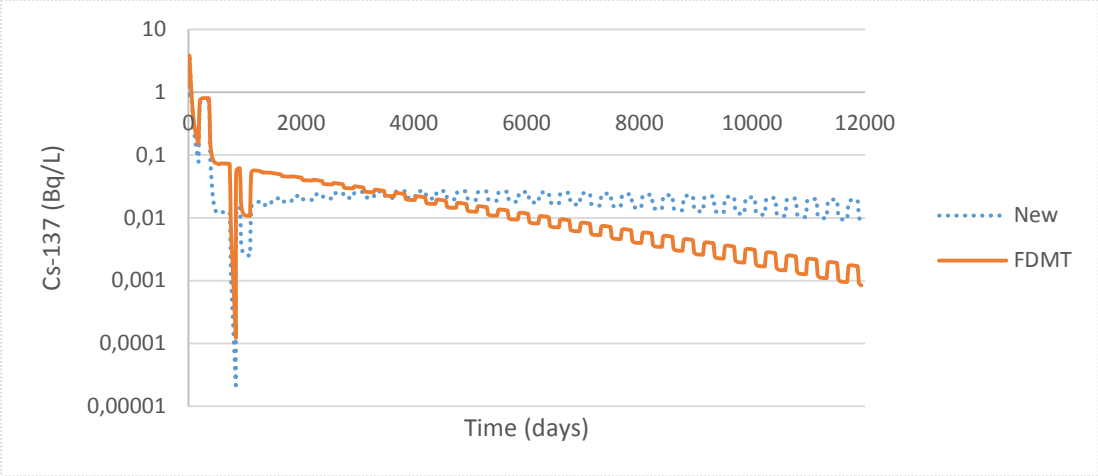

Figure 21. Activity concentrations of ^{137}Cs (Bq/L) in milk with time (days) simulated using 2 models : 'New' fuel-particle soil model (dashed blue line) and FDMT (solid orange line); for Scenario 6 (South, high pH). Deposition ^{137}Cs = 1 kBq/m^2 to soil, 50 kBq/m^2 to vegetation.

The simulations demonstrate that activity concentrations in grass and milk are dominated by initial processes such as the deposition to and interception by vegetation. Even for a rather modest deposition (to grass) of 50 Bq/m^2 aerosol (as used in these simulations), the activity concentrations in the first month or so are orders of magnitude greater than levels associated with long term processes, i.e. release of radionuclides from particles and root uptake.

The influence of including particles in the model only really comes into play at late stages (around 4000 days) in the simulation, at which stage the original soil model in FDMT predicts substantial losses from the system. This is in agreement with the suggestion of (Salbu et al., 1994) that "*the long-term transfer would be underestimated if mobilization of radionuclides from fuel particles due to weathering is not taken into account*.''

The results are also congruent with the work of (Smith, 2009) who, in applying a simpler food-chain model for different fuel particle fractions and particle leaching rates, demonstrated that for low leaching rates ($T_{1/2}$ = 17.3 y), ^{137}Cs activity concentrations in milk associated with a high fraction of deposited FPs would be predicted to be substantially greater than values associated with a low (or negligible) fraction of deposited FPs once 5 years (ca. 2000 days) had elapsed.

4.8 Uncertainties and limitations with the approaches

One way of reconsidering the above-mentioned scenario for the soil-grass-cow system would be to input 1 kBq/m^2 onto vegetation, in line with a conventional approach using the FDMT model, which would clearly lead to correspondingly greater ^{137}Cs levels in the food-chain. Smith (2009), concluded that the time integrated committed effective dose for people (for a 20 year period) is reduced by a substantial fraction for ^{137}Cs for a case in which a large proportion of radioactive particles are present compared to a case where radionuclides are all deposited in available form. This is congruent with our study. However, Smith also recognised that substantial uncertainties in his analysis remained, not least the ingestion of radioactive particles either by farm animals or directly by humans, and conceded that the initial ''spike'' in activity concentrations due to ingestion by animals of radioactivity adhering to plant surfaces was not modelled (2009). Similar caveats exist for our model. Although the aerosol

fraction of the initial deposited activity on vegetation can be modelled, we currently have no way of simulating these processes for FPs. The underlying experimental data providing information on interception (under dry and wet deposition conditions) and subsequent weathering from plant surfaces are simply unavailable or too sparse to parameterise the model convincingly. Moreover, applying models to account for entry of particles into the food-chain *via* ingestion by animals is scope for future work. With reference to the initially elevated activity concentrations in the food chain following a deposition event it would seem advisable to focus more on these initial-phase processes.

The question of 'which food products are sensitive to particles deposited?' cannot be answered in detail from the models as applied. From the analysis conducted above in relation to the soil-grass-cow milk pathway, it seems quite evident that the initial period is really the dominant phase when we might be most concerned with sensitivity of food products to particles. For this to be considered robustly, the model needs to be parameterized with respect to processes such as deposition, interception and retention in the canopy. Over the longer phase, i.e. years post deposition and in the simplest terms, the food products that may be most sensitive are those that exhibit the highest soil to plant transfer. This may seem to be an avoidance of the original question but, in truth, reflects our current inability to dispense with the use of (steady-state) soil to plant transfer factors, with their provenance in large underpinning empirical datasets, for making long-term prognoses. To reiterate, the developments made in this work have been limited to simulating the behavior of particles in soil and modelling the transfer of radionuclides into the food-chain has relied on existing methodologies (from the FDMT model). Without the possibility to determine the effect that the characteristics of crop and forage surfaces have on the interception and retention of particles, *per se*, it was not practicable to establish which specific vegetation types (and associated foodstuffs such as milk from cows ingesting contaminated grass following particle deposition) may be most sensitive to the presence of particles.

The limitations that we encountered are not unique and contain the same caveats as (Smith, 2009) who noted that his calculations '*apply to ingestion of any foodstuff (grains, milk, meat etc.) where the contamination enters the foodstuff via root uptake. It therefore does not account for potential direct ingestion of radioactive particles adhering to foodstuffs, or inadvertent ingestion of radioactive particles in animals' feed*.' Essentially the views of Burkart and Linder (1987) remain valid, i.e. '*Hot particles, highly radioactive particles made up of fission products or actinides and being small enough to become airborne, defy many of the dose models and risk concepts in use by the health physics community. At environmental exposures, both on the level of populations and tissues, dose distributions become very skewed; only few persons or tissue cells being exposed at correspondingly higher levels*.' Although our work has addressed one component of this with respect to an improved simulation of radioactive particles containing ^{137}Cs and ^{90}Sr in soil.

The comparison between the new FP model predictions and empirical datasets leads us to the suggestion that incorporating particles does improve model predictions. This is evidenced both by the fact that the empirical observation of a delayed transfer in ^{13}Cs and ^{90}Sr to crops and other foodstuffs is regenerated when applying the new model and that the predicted activity concentrations of ^{137}Cs and ^{90}Sr in crops using the revised model bear some resemblance to levels measured in the field. However, the effort needs to be focused on the initial phase following deposition. It is still unclear how challenging it will be to adapt and parameterize existing models to account for the presence of particles or, should this be successful, to state, with any confidence, what improvements this might entail.

4.9 How to use the updated models in case of emergency with particle contamination

In the case of radionuclide deposition from any severe nuclear event, radioactive particle contamination should be expected, and it is recommended that laboratories involved in nuclear preparedness are capable of confirming their presence as soon as possible thereby providing valuable source term information to impact assessment models. The presence of submicron - mm sized radioactive particles can rapidly (within a few hours after deposition) be confirmed by 1) digital autoradiography, which will demonstrate heterogeneous distributions on surfaces of contaminated samples such as soil or plants (Salbu et al., 2015), 2) gamma spectrometry, which can demonstrate the presence of refractory fission products such as ^{95}Zr, ^{95}Nb, ^{141,144}Ce, ^{154,155}Eu etc., which indicate the presence of fuel particles (Kashparov et al., 2019), 3) laboratory based micro-XRF or scanning electron microscopy which can be used to characterize the type of fuel particles by means of imaging (morphology, size) and x-ray spectra (Geckeis et al., 2019; Salbu et al., 1994), and 4) subjecting particle contaminated samples (soils, plants etc) to simple leaching experiments (2 M NH_4Ac) in order to determine the exchange fraction of radionuclides in radioactive fallout.

All of these screening analyses can be performed during the first day post deposition. Thus, the results would then be available for use in modelling work in the initial phase of an accident.

5 Conclusions

The inclusion of a model to account explicitly for the presence of particles apparently does make a difference at least in relation to long-term predictions for the activity concentrations of ^{137}Cs and ^{90}Sr in crops and ^{137}Cs in soil, which is in agreement with observations from nuclear accidental sites reported in IAEA (2011) and in the Special Issue of the Journal of Environmental Radioactivity on "Radioactive Particles in the Environment" (2019). The new model accounting for particle behaviour appears to yield less dissimilar results compared to the default model (i.e. FDMT) in the case of predicting ^{90}Sr concentrations in soil although more detailed characterization of environmental conditions and particle composition may temper this conclusion. The new soil particle model appears to predict more realistically the temporal profile of food-chain activity concentrations in the sense that the model reflects a maximum in food-chain activity concentrations occurring many years post deposition. The default model does not provide similarly convincing prognoses. Furthermore, the new model allows account to be taken of parameters that are known to influence environmental transfer such as soil pH and the various components of FP present.

A summary of the difference the implementation of the various models employed make compared to the original FDMT set-up are provided in Table 10 and 11.

Table 10. Comparison of outputs of various models by means of ratios of simulated activity concentrations of ^{137}Cs in soil and crops. NEW refers to the new soil model where U fuel particles are included.

Activity in	**Simulation time**	**FDMT/NEW**	**FDMT*/NEW**		**Comments**
Soil	1 y	0,9	1,0	-	*FDMT without fixation
	10 y	0,4	0,9	-	
	32 y	0,1	0,8	-	
		FDMT/NEW	**FDMT/ABSALOM**	**FDMT/ABSALOM***	
Wheat	1 y	5,1	0,9	6,9	

	10 y	0,6	2,0	15,9	*Absalom with modified rooting zone depth
	32 y	0,1	0,8	6,4	
Grass	1 y	5,2	-	-	-
	10 y	1,0	-	-	-
	32 y	0,1	-	-	-
Milk	1 y	1,1	-	-	-
	10 y	1,1	-	-	-
	32 y	0,1	-	-	-

Table 11. Comparison of outputs of various models by means of ratios of simulated activity concentrations of ^{90}Sr in soil and crops. NEW refers to the new soil model where U fuel particles are included.

Activity in	Simulation time	FDMT/NEW	FDMT/Tag
Soil	1 y	1,0	-
	10 y	0,9	-
	32 y	0,9	-
Wheat	1 y	5,6	1,6
	10 y	1,7	0,5
	32 y	2,2	0,6

Our work shows that, although accounting for FP behaviour in a food-chain transfer model can lead to quite substantial divergence in prognoses for ^{137}Cs levels in grass and milk compared to a 'default' model where this is not accounted for, this may not be critical in a broader perspective unless realistic long-term prognoses are required. For the normal use of FDMT within post-accident decision support systems, it is a moot point as to whether models of the type described above would, in fact, be used to make serious predictions beyond a few years. With this restriction, in terms of the likely time-frame over which predictions would be required, in mind, it appears that little might be gained in accounting for FP behaviour in soil for the short term. In fact, assuming that all deposited activity was as an aerosol (or potentially bioavailable form), with no FP present, would lead to relatively conservative estimates for activity concentrations in the food-chain in the initial (months to years) period. For the given case of ^{137}Cs in the grass-cow-milk system, and within a post-accident decision support system, bearing in mind the putative requirement to provide pessimistic prognoses should there be substantial uncertainty in the analysis, the current FDMT soil model might be considered to be fit-for purpose.

The focus of this work has been on soil models and the impact of considering radioactive particles in such models with regards to transfer. That is, we have ignored the processes involved in the above ground part of the atmosphere-plant-soil system. These would include deposition, interception and subsequent transportation of the released contaminants in the interface of atmosphere and the soil compartment. However, such processes are clearly of great importance when it comes to study the transfer of radioactivity along most food-chains. In fact, JRODOS and ARGOS contain approaches to account for particle sizes and particle densities in the atmospheric dispersion models these systems employ (in considering plume depletion). So, if a particle size distribution of the source term is known, the transport to the point of deposition can be modelled robustly. However, particle behaviour post

deposition is then not accounted for in a subsequent step in the decision support system, i.e. the FDMT model. For the sake of consistency, an approach to consider the aforementioned processes in the atmosphere-plant-soil system, might be desirable. A key challenge here would be the parametrization of the dry deposition velocities for the food-chain transfer models. This parameter is dependent both on the pollutants' characteristic and also deposition surfaces. Giardina and Buffa (2018) have proposed an approach that can be implemented in order to address different particle deposition situations based on considering various categories of pollutants and surfaces. Further work, is planned in this direction.

References

- Absalom, J.P., Young, S.D., Crout, N.M.J., Sanchez, A., Wright, S.M., Smolders, E., Nisbet, A.F., Gillett, A.G., 2001. Predicting the transfer of radiocaesium from organic soils to plants using soil characteristics. J. Environ. Radioact. 52, 31-43.
- Avila, R., Broed, R., Pereira, A., 2005. ECOLEGO - A toolbox for radioecological risk assessment Proceedings of the International Conference on the Protection from the Effects of Ionizing Radiation. International Atomic Energy Agency. IAEA-CN-109/80. pp. 229 - 232, Stockholm.
- Barnett, C.L., Wells, C., Fesenko, S., Tagami, K., Beresford, N.A., 2019. Radionuclide biological half-lives for farm animals. NERC Environmental Information Data Centre.
- Beresford, N.A., Fesenko, S., Konoplev, A., Skuterud, L., Smith, J.T., Voigt, G., 2016. Thirty years after the Chernobyl accident: What lessons have we learnt? Journal of Environmental Radioactivity 157, 77-89.
- Bobovnikova, T.I., Makhon'ko, K.P., Siverina, A.A., Rabotnova, F.A., Gutareva, V.P., Volokitin, A.A., 1991. Physico-chemical forms of radionuclides in the fallout after Chernobyl accident and their transformations in soil. Atomnaya Energiya 71, 449-454.
- Brown, J.E., Avila, R., Barnett, C.L., Beresford, N.A., Hosseini, A., Lind, O.-C., Oughton, D.H., Perez D., Salbu, B., Teien H.C., Thørring, H., 2018. D 9.13 – Improving models and learning from post-Fukushima studies. , Report to EJP-CONCERT; European Joint Programme for the Integration of Radiation Protection Research H2020 – 662287.
- Burkart, W., Linder, H., 1987. Hot particles in the environment: assessment of dose and health detriment. Soz Praventivmed 32, 310-315.
- Camps, M., Rigol, A., Hillier, S., Vidal, M., Rauret, G., 2004. Quantitative assessment of the effects of agricultural practices designed to reduce 137Cs and 90Sr soil-plant transfer in meadows. The Science of the total environment 332, 23-38.
- Devell, L., Tovedal, H., Bergstrom, U., Appelgren, A., Chyssler, J., Andersson, L., 1986. Initial Observations of Fallout from the Reactor Accident at Chernobyl. Nature 321, 192-193.
- Dowdall, M., Brown, J.E., Hosseini, A., Mora Cañadas, J.C., 2012. Impact of legacy enhanced natural radioactivity on human and natural environments., Radionuclides: Sources, Properties and Hazards. Nova Science Publishers, Inc., pp. 171-204.
- Fernandez, J.M., Piault, E., Macouillard, D., Juncos, C., 2006. Forty years of 90Sr in situ migration: importance of soil characterization in modeling transport phenomena. Journal of environmental radioactivity 87, 209-226.
- Fesenko, S.V., Spiridonov, S.I., Sanzharova, N.I., Kuznetsov, V.K., 1998. Enhancement of the EU Decision Support system RODOS and its Customisation for Use in Eastern Europe Russian Institute of Agricultural Radiology and Agroecology, Obninsk, Russia. Progress Report for period 1 July 1997 - 1 October 1998.
- Geckeis, H., Zavarin, M., Salbu, B., Lind, O.C., Skipperud, L., 2019. Environmental Chemistry of Plutonium, in: Clark, D.L., Geeson, D.A., Hanrahan, R.J. (Eds.), Plutonium Handbook, 2 ed. American Nuclear Society, pp. 1979-2118.
- Giardina, M., Buffa, P., 2018. A new approach for modeling dry deposition velocity of particles. Atmospheric Environment 180, 11-22.
- Hird, A.B., Rimmer, D.L., Livens, F.R., 1996. Factors affecting the sorption and fixation of caesium in acid organic soils. European Journal of Soil Science 47, 97-104.

- Hoe, S., Mc Ginnity, P., Charnock, T.W., Gering, F., Andersson, K.G., Astrup, P., 2008 ARGOS CBRN Decision Support System for Nuclear and Radiological Emergency Management. , Proceedings: IRPA 12. The 12th International Congress of the International Radiation Protection Association Buenos Aires, Argentina.
- Hou, X.L., Fogh, C.L., Kucera, J., Andersson, K.G., Dahlgaard, H., Nielsen, S.P., 2003. Iodine-129 and Caesium-137 in Chernobyl contaminated soil and their chemical fractionation. Science of The Total Environment 308, 97-109.
- IAEA, 2006. Environmental Consequences of the Chernobyl Accident and their Remediation: Twenty Years of Experience; Report of the Chernobyl Forum Expert Group 'Environment', International Atomic Energy Agency, Vienna.
- IAEA, 2010. Handbook of Parameter Values for the Prediction of Radionuclide Transfer in Terrestrial and Freshwater Environments, IAEA Technical Report Series No. 472. International Atomic Energy Agency, Vienna.
- Ivanov, Y.O., Khomutinin, Y.V., 2015. Mathematical modelling of dynamics of 90Sr and 137Cs migration in components of agrocenosises soil-plant cover at the late phase of radiation accident. I. Construction of the model and its parametrization. Nuclear Physics and Atomic Energy 16, 169-176.
- Kashparov, V., Salbu, B., Levchuk, S., Protsak, V., Maloshtan, I., Simonucci, C., Courbet, C., Nguyen, H.L., Sanzharova, N., Zabrotsky, V., 2019. Environmental behaviour of radioactive particles from chernobyl. Journal of environmental radioactivity 208-209, 106025-106025.
- Kashparov, V., Yoshchenko, V., Levchuk, S., Tschiersch, J., Wagenpfeil, F., 2000a. Application of the Method of Repeated Mixing to Non-Uniformly Contaminated Bulky Samples. An International Journal Dealing with All Aspects and Applications of Nuclear Chemistry 246, 165-172.
- Kashparov, V.A., 2009a. Radioecological significance of a fuel component of Chernobyl radioactive fallout, Ukraine, pp. 5-22.
- Kashparov, V.A., 2009b. Radioecological significance of a fuel component of Chernobyl radioactive fallout. , Problems of Chernobyl exclusion zone, pp. 5-22.
- Kashparov, V.A., Ahamdach, N., Zvarich, S.I., Yoschenko, V.I., Maloshtan, I.M., Dewiere, L., 2004a. Kinetics of dissolution of Chernobyl fuel particles in soil in natural conditions. Journal of Environmental Radioactivity 72, 335-353.
- Kashparov, V.A., Ahamdach, N., Zvarich, S.I., Yoschenko, V.I., Maloshtan, I.M., Dewiere, L., 2004b. Kinetics of dissolution of Chernobyl fuel particles in soil in natural conditions. J Environ Radioact 72, 335-353.
- Kashparov, V.A., Ivanov, Y.A., Zvarisch, S.I., Protsak, V.P., Khomutinin, Y.V., Kurepin, A.D., Pazukhin, E.M., 1996. Formation of hot particles during the Chernobyl nuclear power plant accident. Nuclear Technology 114, 246-253.
- Kashparov, V.A., Lundin, S.M., Zvarych, S.I., Yoshchenko, V.I., Levchuk, S.E., Khomutinin, Y.V., Maloshtan, I.M., Protsak, V.P., 2003. Territory contamination with the radionuclides representing the fuel component of Chernobyl fallout. Sci Total Environ 317, 105-119.
- Kashparov, V.A., Oughton, D.H., Protsak, V.P., Zvarisch, S.I., Levchuk, S.E., 1999a. Kinetics of fuel particle weathering and 90 Sr mobility in the Chernobyl 30 km exclusion zone Health Physics 76, 251-259.
- Kashparov, V.A., Oughton, D.H., Zvarich, S.I., Protsak, V.P., Levchuk, S.E., 1999b. Kinetics of fuel particle weathering and Sr-90 mobility in the Chernobyl 30-km exclusion zone. Health Physics 76, 251-259.

- Kashparov, V.A., Protsak, V.P., Ahamdach, N., Stammose, D., Peres, J.M., Yoshchenko, V.I., Zvarich, S.I., 2000b. Dissolution kinetics of particles of irradiated Chernobyl nuclear fuel: influence of pH and oxidation state on the release of radionuclides in the contaminated soil of Chernobyl. Journal of Nuclear Materials 279, 225-233.
- Levdin, I., Trybushnyi, D., Zheleznyak, M., Raskob, W., 2010 RODOS re-engineering: aims and implementation details. . Radioprotection, 45 (Enhancing Nuclear and Radiological Emergency Management and Rehabilitation: Key Results of the EURANOS European Project.) S181–S189.
- Müller, H., Gering, F., Pröhl, G., 2004. Model description of the Terrestrial Food Chain and Dose Module FDMT in RODOS PV 6.0., RODOS(RA3)-TN(03)06, Report (version 1.1, 18.02.2004).
- Müller, H., Pröhl, G., 1993 ECOSYS-87: A dynamic model for assessing radiological consequences of nuclear accidents. Health Phys. 64 232-252.
- Otreshko, L.M., Levchuk, S.E., Yoshchenko, V.I., 2014. Activity concentration of 90Sr in grain on fuel traces of Chernobyl radioactive fallout. Nuclear Physics and Atomic Energy 15, 171-177.
- Oughton, D.H., Salbu, B., Riise, G., Lien, H., Nøren, A., 1992. Radionuclide mobility and bioavailability in Norwegian and Soviet soils. . Analyst 117, 481-486.
- Prorok, V.V., Dacenko, O.I., Bulavin, L.A., Poperenko, L.V., White, P.J., 2016. Mechanistic interpretation of the varying selectivity of Cesium-137 and potassium uptake by radish (Raphanus sativus L.) under field conditions near Chernobyl. Journal of Environmental Radioactivity 152, 85-91.
- Raskob, W., Almahayni, T., Beresford, N.A., 2018. Radioecology in CONFIDENCE: Dealing with uncertainties relevant for decision making. Journal of Environmental Radioactivity 192, 399-404.
- Riise, G., Bjornstad, H.E., Lien, H.N., Oughton, D.H., Salbu, B., 1990. A study of radionuclide association with soil components using a sequential extraction procedure. Journal of radioanalytical and Nuclear Chemistry, Articles 142, 531-538.
- Salbu, B., 1988. Radionuclides associated with colloids and particles in rainwaters, Oslo, Norway, in: von Philipsborn, H., Steinh„user, F. (Eds.), Hot particles from the Chernobyl Fallout. Bergbau - und Industrimuseum, Theuern, pp. 83-84.
- Salbu, B., Kashparov, V., Lind, O.C., Garcia-Tenorio, R., Johansen, M.P., Child, D.P., Roos, P., Sancho, C., 2018. Challenges associated with the behaviour of radioactive particles in the environment. Journal of Environmental Radioactivity 186, 101-115.
- Salbu, B., Krekling, T., Oughton, D.H., Østby, G., Kashparov, V.A., Brand, T.L., Day, J.P., 1994. Hot particles in accidental releases from Chernobyl and Windscale nuclear installations. Analyst 119
- Salbu, B., Lind, O., Skipperud, L., 2004. Radionuclide speciation and its relevance in environmental impact assessments. Journal of Environmental Radioactivity 74, 233-242.
- Salbu, B., Skipperud, L., Lind, O.C., 2015. Sources Contributing to Radionuclides in the Environment: With Focus on Radioactive Particles, in: Walther, C., Gupta, D.K. (Eds.), Radionuclides in the Environment. Springer International Publishing, Cham, pp. 1-36.
- Shevchenko, S.V., 2004. On the uncertainty in activity measurements for samples containing "hot particles". Applied Radiation and Isotopes 61, 1303-1306.
- Smith, J.T., 2009. The influence of hot particle contamination on (90)Sr and (137)Cs transfers to milk and on time-integrated ingestion doses. Journal of environmental radioactivity 100, 322-328.
- Smolders, E., Van den Brande, K., Merckx, R., 1997. Concentration of 137Cs and K in soil solution predicts the plant availability of 137Cs in soils. Environ. Sci. Technol. 31, 3432 –3438.
- Staudt, C., 2016 HARMONE Database with values for geographically dependent parameters., Deliverable OPERRA Deliverable D5.36. EC, Brussels.

- Tarsitano, D., Young, S.D., Crout, N.M., 2011. Evaluating and reducing a model of radiocaesium soil-plant uptake. Journal of environmental radioactivity 102, 262-269.
- Thørring, H., Dyve, J., Hevrøy, T., Lahtinen, J., Liland, A., Montero, M., Real, A., Simon-Cornu, M., Trueba, C., 2016 Sets of improved parameter values for Nordic and Mediterranean ecosystems for Cs-134/137, Sr-90, I-131 with justification text. , COMET Deliverable IRA-Human-D3. EC, Brussels
- Vandebroek, L., Van Hees, M., Delvaux, B., Spaargaren, O., Thiry, Y., 2012. Relevance of Radiocaesium Interception Potential (RIP) on a worldwide scale to assess soil vulnerability to 137Cs contamination. Journal of environmental radioactivity 104, 87-93.
- Vidal, M., Roig, M., Rigol, A., Llaurado, M., Rauret, G., Wauters, A., Elsen, A., Cremers, A., 1995. Two approaches to the study of radiocaesium partitioning and mobility in agricultural soils form the Chernobyl area. Analyst 120 1785-1791.
- Zhurba, M., Kashparov, V., Ahamdach, N., Salbu, B., Yoschenko, V., Levchuk, S., 2009. The "hot particles" data base, in: Oughton, D.H., Kashparov, V. (Eds.), Nato Sci Peace Secur, pp. 187-195.

Annex

Table S 1. The results of the monitoring of radioactive contamination of soil and grain in the Ivankovsky district in 2011. Data highlighted in grey were used for evaluating the model outputs in the present work.

No	Setlement	Plant	Sampling points location		pH	Ca, meq per 100g of soil	Activity concentration radionucludes in soil, Bq/kg				Activity concentration radionucludes in grain, Bq/kg			
			latitude	longitude			^{137}Cs	STD, 95%	^{90} Sr	STD, 95%	^{137}Cs	STD, 95%	^{90} Sr	STD, 95%
1	Dytiatky	oat (*Avéna*)	51.11178	30.12102	5.47	1.53	210	21	68	10.9	13	1.0	**39**	5
		rye (*Secále cereále*)	51.11192	30.12335	6.4	3.21	200	18	59	10	4	0.9	18	4
		oat (*Avéna*)	51.11169	30.1242	6.38	3.72	170	17	54	8.6	6.8	1.3	**31**	3
5	Gornostaypil'	rye (*Secále cereále*)	51.07677	30.25922	5.62	4.23	207	20.7	86	10.3	<2		4	2
		oat (*Avéna*)	51.07633	30.2592	6.01	5.32	148	14.8	60	7.2	<1		5	1
		rye (*Secále cereále*)	51.07543	30.28642	6.44	5.45	185	18.5	88	8.8	2	0.7	5	1
6	Zorin	rye (*Secále cereále*)	51.05131	30.19496	5.65	3.28	130	13	58	9.3	<1		13	2
		oat (*Avéna*)	51.05834	30.18957	5.74	3.92	140	14	62	9.3	6	1.0	14	1
8	Prybirsk	wheat (*Tríticum*)	51.02506	30.05313	6.61	3.09	160	16	65	7.8	2.3	0.5	**32**	4
		oat (*Avéna*)	51.02548	30.05278	5.9	0.91	109	10.9	30	9	8	1.1	**61**	5
		wheat (*Tríticum*)	51.00673	29.99022	7.6	2.3	70	8.4	20	6	<0.2		4	1
		rye (*Secále cereále*)	50.99538	29.96932	5.98	1.63	120	12	24	9.6	3.2	1.1	15	2
		rye (*Secále cereále*)	50.9867	29.95449	6.31	3.18	158	15.8	32	9.6	2.6	0.9	11	2

Table S 2. The results of the monitoring of radioactive contamination of soil and grain in the Ivankovsky district in ***2012.*** Data highlighted in grey were used for evaluating the model outputs in the present work.

No	Setlement	Plant	Sampling points location		pH	Ca, meq per 100g of soil	Activity concentration radionucludes in soil, Bq/kg				Activity concentration radionucludes in grain, Bq/kg			
			latitude	longitude			^{137}Cs	STD, 95%	^{90}Sr	STD, 95%	^{137}Cs	STD, 95%	^{90}Sr	STD, 95%
1	Dytiatky	rye (*Secále cereále*)	51.11168	30.13565	5.57	0.94	170	19	29	6	<3		**34**	3
		oat (*Avéna*)	51.11281	30.12245	6.4	3.21	208	21	59	12	8	3	**21**	3
		rye (*Secále cereále*)	51.11112	30.12083	5.93	1.94	242	24	74	15	8	3	**44**	3
2	Karpylivka	oat (*Avéna*)	50.585984	30.482713	5.57	1.86	47	7	25	5	<1		**50**	4
		rye (*Secále cereále*)	50.592003	30.482428	5.64	4	69	7	26	5	<3		6	2
5	Gornostaypil'	rye (*Secále cereále*)	51.06876	30.22932	7.2	1.75	184	18	56	11	<4		14	1
8	Prybirsk	rye (*Secále cereále*)	51.025024	30.053318	6.2	2.2	170	14	19	4	<4		12	2
		rye (*Secále cereále*)	51.022467	30.048511	6.26	1.97	156	17	32	6	6	2	19	2
		rye (*Secále cereále*)	51.02204	30.048033	5.9	0.91	171	19	30	6	<4		16	2
		wheat (*Tríticum*)	51.011471	30.000256	8.07	2.28	136	15	43	9	<3		**21**	2
		wheat (*Tríticum*)	51.010592	30.001401	5.68	2.5	151	15	27	5	<4		**52**	4
		rye (*Secále cereále*)	51.006756	29.986457	6.32	1.86	114	11	33	7	<4		16	1
11	Pyrogovychi	wheat (*Tríticum*)	51.00612	29.9889	7.6	2.3	123	12	20	4	<4		**23**	2
		wheat (*Tríticum*)	50.994338	29.968952	5.98	1.63	120	14	24	5	<3		15	2
		wheat (*Tríticum*)	50.98716	29.95564	6.31	3.18	122	15	32	6	<4		**20**	2

Table S 3. The results of the monitoring of radioactive contamination of soil and grain in the Ivankovsky district in 2013. Data highlighted in grey were used for evaluating the model outputs in the present work.

No	Setlement	Plant	Sampling points location		pH	Ca, meq per 100g of soil	Activity concentration radionucludes in soil, Bq/kg				Activity concentration radionucludes in grain, Bq/kg			
			latitude	longitude			^{137}Cs	STD, 95%	^{90}Sr	STD, 95%	^{137}Cs	STD, 95%	^{90}Sr	STD, 95%
1	Dytiatky	rye (*Secále cereále*)	51.112354	30.124136	6.82	3.38	200	10	26	5	< 12		**55**	7
		oat (*Avéna*)	51.111546	30.122870	5.84	2.81	178	9	45	9	16	4	**40**	5
5	Gornostaypil'	oat (*Avéna*)	51.075759	30.285121	6.25	5.69	230	12	85	16	< 16		**39**	5
6	Zorin	oat (*Avéna*)	51.058380	30.189570	5.65	3.38	140	7	50	10	12	6	**40**	6
8	Prybirsk	oat (*Avéna*)	51.024500	30.054150	5.54	3.19	210	11	56	11	24	11	**46**	6
		oat (*Avéna*)	51.022164	30.049180	5.16	1.88	165	8	72	13	25	8	**55**	7
		oat (*Avéna*)	51.021745	30.048110	5	2.31	136	7	51	10	< 6		**36**	5
		oat (*Avéna*)	51.006513	29.993307	5.64	1.69	145	7	40	8	< 12		**59**	8
11	Pyrogovychi	rye (*Secále cereále*)	50.995138	29.967769	5.82	1.81	117	6	17	4	< 12		**55**	7
		rye (*Secále cereále*)	50.985038	29.957754	5.18	1.56	124	6	27	6	26	12	**50**	6
		rye (*Secále cereále*)	50.992318	29.952222	5.21	5.25	115	6	32	9	< 11		**24**	3

Table S 4. The results of the monitoring of radioactive contamination of soil and grain in the Ivankovsky district in 2014. Data highlighted in grey were used for evaluating the model outputs in the present work.

No	Setlement	Plant	Sampling points location		pH	Ca, meq per 100g of soil	Activity concentration radionucludes in soil, Bq/kg				Activity concentration radionucludes in grain, Bq/kg			
			latitude	longitude			^{137}Cs	STD, 95%	^{90}Sr	STD, 95%	^{137}Cs	STD, 95%	^{90}Sr	STD, 95%
1	Dytiatky	oat (*Avéna*)	51.1118	30.13209	6	3.2	186	10	65	8	<10		**23**	2
		oat (*Avéna*)	51.11216;	30.12701	5	1.2	154	10	32	9	20	4	**48**	4
3	Pisky	rye (*Secále cereále*)	51.10093	30.02399	5.8	2	155	11	64	8	<10		**31**	3
		rye (*Secále cereále*)	51.08856	30.01544	7.8	3.6	173	10	61	8	<4		10	1
4	Domanivka	rye (*Secále cereále*)	51.08298	29.98461	6.7	2.6	118	10	23	10	<7		17	2
		rye (*Secále cereále*)	51.07032	29.97194	5.9	2.2	109	11	27	11	<9		18	2
5	Gornostaypil'	rye (*Secále cereále*)	51.07869	30.24033	5.2	3.8	117	11	37	9	<4		11	1
		rye (*Secále cereále*)	51.08173	30.26276	5.8	3	193	10	54	8	<10		15	2
6	Zorin	oat (*Avéna*)	51.057881	30.18909	5.5	3.4	123	11	39	9	<3		16	2
8	Prybirsk	oat (*Avéna*)	51.007291	29.983915	5.1	1.8	156	10	31	9	13	10	**28**	3
		oat (*Avéna*)	51.01108	30.00093	4.8	0.6	140	10	17	9	<10		**58**	5
		oat (*Avéna*)	51.00325	29.98328	4.9	1.2	136	10	20	10	<5		**24**	2
9	Rusaky	rye (*Secále cereále*)	51.03102	29.95508	5.4	2.6	121	10	29	8	<8		18	2
		oat (*Avéna*)	51.00837	29.9522	4.9	1.2	107	11	17	9	<9		19	2
10	Fedorivka	wheat (*Tríticum*)	50.9786	29.89902	6.8	3.8	85	11	22	9	<9		5	1
11	Pyrogovychi	rye (*Secále cereále*)	50.98976	29.95937	5.1	2.4	110	11	22	10	<10		13	1

Table S 5. The results of the monitoring of radioactive contamination of soil and grain in the Ivankovsky district in 2015. Data highlighted in grey were used for evaluating the model outputs in the present work.

No	Setlement	Plant	Sampling points location		pH	Ca, meq per 100g of soil	Activity concentration radionucludes in soil, Bq/kg				Activity concentration radionucludes in grain, Bq/kg			
			latitude	longitude			^{137}Cs	STD, 95%	^{90}Sr	STD, 95%	^{137}Cs	STD, 95%	^{90}Sr	STD, 95%
1	Dytiatky	oat (*Avéna*)	51.11219	30.12688	4.4	0.88	36	5	85	9	<7		**50**	4.0
		oat (*Avéna*)	51.11152	30.12682	5.1	2.31	56	8	678	68	<9		**41**	3.3
3	Pisky	rye (*Secále cereále*)	51.09655	30.02161	4.9	2.05	87	13	435	44	7	3	**25**	2.5
4	Domanivka	rye (*Secále cereále*)	51.08246	29.98303	5.1	2	25	4	107	11	<6		**35**	3.2
5	Gornostaypil'	rye (*Secále cereále*)	51.07598	30.2412	5.1	2.63	74	11	210	21	5	2	16	1.7
		rye (*Secále cereále*)	51.08083	30.2625	6.5	5.36	75	11	197	20	<1		6	0.9
8	Prybirsk	wheat (*Tríticum*)	51.00761	29.9539	5.3	2.42	44	7	130	13	<2		**27**	2.1
10	Fedorivka	wheat (*Tríticum*)	50.98161	29.90288	6.5	5.1	20	3	95	10	<0.6		3.0	0.7
		wheat (*Tríticum*)	50.98646	29.89642	6.5	5.4	18	3	110	11	1	0.33	2.0	0.5
		wheat (*Tríticum*)	50.9843	29.892	6.4	4.8	19	3	85	9	1	0.4	4.0	0.8
11	Pyrogovychi	oat (*Avéna*)	50.9903	29.9539	5.2	3.13	29	4	110	11	4	1.6	4	0.7
		oat (*Avéna*)	50.98594	29.9545	4.9	2.3	22	3	184	18	<3		4	0.7

Table S 6. The results of the monitoring of radioactive contamination of soil and grain in the Ivankovsky district in 2016. Data highlighted in grey were used for evaluating the model outputs in the present work.

No	Setlement	Plant	Sampling points location		pH	Ca, meq per 100g of soil	Activity concentration radionucludes in soil, Bq/kg				Activity concentration radionucludes in grain, Bq/kg			
			latitude	longitude			^{137}Cs	STD, 95%	^{90}Sr	STD, 95%	^{137}Cs	STD, 95%	^{90}Sr	STD, 95%
1	Dytiatky	oat (*Avéna*)	51.11003	30.12112	4.60	3.69	152	15	55	5	8.4	2		
5	Gornostaypil'	rye (*Secále cereále*)	51.0741	30.24143	5.37	3.50	195	20	78	6	3	1	14.6	1.6
		rye (*Secále cereále*)	51.0803	30.26238	5.60	3.97	200	20	49	4	<1		9.8	0.9
		oat (*Avéna*)	51.07918	30.28535	5.77	5.00	164	16	65	5	<1			
		rye (*Secále cereále*)	51.07803	30.29578	6.47	4.48	210	21	44	4	3	1	10.0	1.2
		rye (*Secále cereále*)	51.0836	30.303	5.20	1.81	67	7	26	2	2	1	13.0	1.5
		rye (*Secále cereále*)	51.078433	30.30537	5.30	1.25	131	13	37	3	8	2	14.4	1.6
		тритікале	51.07432	30.2762	5.35	6.00	151	15	48	4	<0.7		9.0	1.2
8	Prybirsk	rye (*Secále cereále*)	50.9918	29.96368	5.22	2.56	149	15	37	3	<1		13.5	1.3
		rye (*Secále cereále*)	50.99413	29.96773	5.32	1.69	119	12	23	2	<3		15.6	1.4

Table S 7. The results of the monitoring of radioactive contamination of soil and grain in the Ivankovsky district in 2017. Data highlighted in grey were used for evaluating the model outputs in the present work.

No	Setlement	Plant	Sampling points location		pH	Ca, meq per 100g of soil	Activity concentration radionucludes in soil, Bq/kg				Activity concentration radionucludes in grain, Bq/kg			
			latitude	longitude			^{137}Cs	STD, 95%	^{90} Sr	STD, 95%	^{137}Cs	STD, 95%	^{90} Sr	STD, 95%
1	Dytiatky	oat (*Avéna*)	51.10871	30.120608			220	22	70	11	7.0	1.3	10	2
5	Gornostaypil'	wheat (*Tríticum*)	51.08479	30.2368	5.1	4.4	182	15	77	7	1.2	0.2	11	3
		wheat (*Tríticum*)	51.08081	30.240508	4.7	4.65	170	10	60	5	1.9	0.4	8	2
		wheat (*Tríticum*)	51.08329	30.261568	5	2.5	177	16	45	4	1.3	0.4	15	4
		oat (*Avéna*)	51.07452	30.27465	5.2	6.56	110	8	40	4	0.7	0.3	8	2
		wheat (*Tríticum*)	51.08645	30.282738	5.3	2.4	118	8	24	2	0.6	0.2	10	3
		wheat (*Tríticum*)	51.08713	30.29328	4.6	1.49	148	12	34	3	2.4	0.4	**25**	5
		oat (*Avéna*)	51.07847	30.296146	5.2	2.32	200	16	104	9	2.8	0.4	**35**	7
		Triticale (*Triticosecale*)	51.07883	30.294956	4.5	1.8	200	16	104	9	3.0	1.2	17	5
		oat (*Avéna*)	51.07701	30.326835	4.5	1.8	51	4	17	2	2.1	0.5	15	5
6	Zorin	rye (*Secále cereále*)	51.05822	30.178118	5.1	2.24	162	11	39	4	10.0	0.7	**22**	4
		rye (*Secále cereále*)	51.0496	30.189107	4.9	2.41	121	10	26	2	1.1	0.2	18	4
		rye (*Secále cereále*)	51.05175	30.196053	4.9	3.24	117	8	32	3	1.0	0.3	12	4
		rye (*Secále cereále*)	51.0623	30.196201	4.5	2.66	180	11	34	3	1.1	0.4	**22**	6
		rye (*Secále cereále*)	51.06721	30.215659	4.6	2.66	100	9	25	2	4.1	0.8	17	4
9	Rusaky	wheat (*Tríticum*)	51.02784	29.957024	3.9	2.32	119	7	26	2	0.9	0.5	14	3
		rye (*Secále cereále*)	51.03663	29.952454	4.5	3.24	67	4	19	2	1.2	0.4	13	3
		wheat (*Tríticum*)	51.04208	29.959461	4.8	2.08	77	6	26	2	4.2	0.4	16	4

Table S 8. The results of the monitoring of radioactive contamination of soil and grain in the Ivankovsky district in 2018. Data highlighted in grey were used for evaluating the model outputs in the present work.

No	Setlement	Plant	Sampling points location		pH	Ca, meq per 100g of soil	Activity concentration radionucludes in soil, Bq/kg				Activity concentration radionucludes in grain, Bq/kg			
			latitude	longitude			^{137}Cs	STD, 95%	^{90}Sr	STD, 95%	^{137}Cs	STD, 95%	^{90}Sr	STD, 95%
1	Dytiatky	barley (*Hórdeum*)	51.11201	30.11556		3.8	11.13	7	65	5.4	3.4	0.374	**24**	3.84
5	Gornostaypil'	oat (*Avéna*)	51.07750	30.33079		1.8	4.75	5	26	2.0	3	0.36	**25**	4.25
		oat (*Avéna*)	51.04409	30.57603		2.03	10.8	6	45.2	4.0	8	0.8	**65**	11.05
		rye (*Secále cereále*)	51.08446	30.29047		1.9	6.96	6	31.2	3.0	1	0.5	**26**	4.68
		oat (*Avéna*)	51.07913	30.28509		4.7	10.86	6	36.5	3.0	4	0.4	10	3
		oat (*Avéna*)	51.07818	30.28600		5.8	8.16	6	47.7	4.0	3	0.3	8	2.08
7	Orane	rye (*Secále cereále*)	51.06966	30.16647		1.1	10.2	6	30	2.4	8	0.64	**28**	4.2

References

- Kashparov, V.; Levchuk, S.; Zhurba, M.; Protsak, V.; Khomutinin, Yu.; Beresford, N.A.; Chaplow, J.S. 2018. Spatial datasets of radionuclide contamination in the Ukrainian Chernobyl Exclusion Zone. Earth System Science Data (ESSD). 10, 339-353. https://doi.org/10.5194/essd-10-339-2018
- Kashparov, V. A.; Levchuk, S. E.; Otreshko, L. N.; Maloshtan, I. M., 2013. Contamination of Agricultural Production with ^{90}Sr in Ukraine at the Late Phase of the Chernobyl Accident. Radiation Biology. Radioecology. 53(6), 639-650 (In Russian).
- Otreshko, L.N., Levchuk, S.., Yoshchenko, V.I., 2014. Concentration of ^{90}Sr in grain on fuel traces of the Chernobyl radioactive fallout (in Ukrainian). Nucl. Phys. At. Energy 15, 171–177.